Journal of Sedimentary Research

Journal of Sedimentary Research, 2018, v. 88, 942–959
Research Article
DOI: http://dx.doi.org/10.2110/jsr.2018.50

THE TECTONICALLY CONTROLLED SAN GABRIEL CHANNEL–LOBE TRANSITION ZONE, CATALINA BASIN, SOUTHERN CALIFORNIA BORDERLAND

KATHERINE L. MAIER,*[1] EMILY C. ROLAND,[2] MAUREEN A.L. WALTON,[1] JAMES E. CONRAD,[1] DANIEL S. BROTHERS,[1] PETER DARTNELL,[1] AND JARED W. KLUESNER[1]

[1]*U.S. Geological Survey, Pacific Coastal and Marine Science Center, 2885 Mission Street, Santa Cruz, California 95060, U.S.A.*
[2]*University of Washington, School of Oceanography, 1501 NE Boat Street, Seattle, Washington 98195, U.S.A.*
e-mail: Katherine.L.Maier@gmail.com

ABSTRACT: **High-resolution geophysical data across the Catalina Basin, offshore southern California, USA, reveal a complex channel–lobe transition zone (CLTZ) and provide an opportunity to characterize an entire seafloor CLTZ in a tectonically active and confined-basin setting. The seafloor morphology, distribution of depositional and erosional features, and location of depocenters in the CLTZ are controlled by shifting confinement and seafloor gradient related to inherited basement structures, active faults, and basin margins. Below a Holocene hemipelagic drape, the Catalina Basin is dominated by CLTZ and lobe sedimentation from the San Gabriel Channel, with lesser accumulations from local sediment sources limited to basin margins. The San Gabriel Channel is structurally confined as it enters the Catalina Basin and appears unable to avulse; it continues into the basin as a channel that rapidly widens, decreases in relief, and becomes scoured at its margins. A CLTZ is imaged between the confined San Gabriel channel and its terminal lobes deposited > 50 km into the basin. Narrow, apparently disconnected channels with knickpoints occur throughout the proximal and mid-CLTZ and are concentrated near basement highs and basin-bounding Quaternary-active dextral strike-slip faults. A field of small-scale erosional crescent-shaped scours (∼ 100 m length, ∼ 200 m width, up to ∼ 10 m relief across ∼ 30 km^2 region) occurs above a partially buried basement high that creates perturbations in seafloor gradient. Likewise, above a buried basement structure that locally increases seafloor gradient (up to 0.4°), the distal CLTZ may contain sediment waves (∼ 2–4 m wave height and ∼ 200–300 m wavelength) that are smaller than many other CLTZ examples. This study of the San Gabriel CLTZ in Catalina Basin provides high-resolution geophysical data coverage of a complete CLTZ and illustrates a tectonically controlled end-member CLTZ from the modern seafloor.**

INTRODUCTION

Submarine fans are composite sediment accumulations at the distal ends of deep-sea canyons and channels (e.g., Normark 1970), and they can provide sediment sinks, serve as hydrocarbon reservoirs, and host records of climate and tectonics. Questions of how sediments are transported into the deep sea, accumulate in submarine fans, sculpt seafloor morphology, and change from channelized to unchannelized deposits have motivated decades of research (e.g., Shepard et al. 1969; Normark 1970; Mutti and Normark 1987; Richards and Bowman 1998; Wynn et al. 2002; Prélat et al. 2010; Maier et al. 2011; Carvajal et al. 2017, and many others). In some deep-sea depositional systems, a well-defined, confined channel and terminal lobes are separated by a complex region of erosion, bypass, and deposition, referred to as the channel–lobe transition zone (CLTZ) (e.g., Mutti and Normark 1987; Wynn et al. 2002). CLTZs are principal elements and relatively common features of turbidite deep-sea depositional systems worldwide, and thus, comparison of turbidite depositional systems requires detailed mapping and characterization of CLTZs (Mutti and Normark 1987). In particular, the CLTZ has been highlighted as a region of importance for records of sediment-density-flow processes across areas of changing confinement, which can influence resulting stratigraphy, lithology, geometry, and lateral connectivity of sand deposits in submarine fans (e.g., Normark et al. 1979; Mutti and Normark 1987; Shanmugam and Moiola 1991; Wynn et al. 2002; Bernhardt et al. 2011; Postma et al. 2016; Carvajal et al. 2017). Detailed characterization of CLTZs, including morphology and shallow stratigraphy, is needed to refine the recognition criteria and conceptual models of CLTZ features (e.g., Wynn et al. 2002), and to successfully target sampling of submarine-fan records (e.g., Normark et al. 1998; Romans et al. 2009).

Despite the importance of CLTZs, few modern seafloor examples have been comprehensively characterized with high-resolution geophysical imaging across an entire CLTZ (e.g., Wynn et al. 2002; Carvajal et al. 2017). Deep-sea fans and CLTZs on the modern seafloor have been challenging to study because of their large size, often remote locations, and water depths of hundreds to thousands of meters that limit resolution of traditional datasets (e.g., Shepard et al. 1969; O'Connell and Normark 1986; Mutti and Normark 1987; Twitchell et al. 1992; Piper and Normark 2001; Normark et al. 2009b; Carvajal et al. 2017). This has led to imaging across parts of seafloor CLTZs and composite conceptual models of CLTZ features (e.g., Wynn et al. 2002; Bonnel et al. 2005). As Dorrell et al.

* Present Address: Monterey Bay Aquarium Research Institute, 7700 Sandholdt Road, Moss Landing, California 95039, U.S.A.

Published Online: August 2018
 1527-1404/18/088-942/

(2016) highlighted, modern seafloor examples from tectonically active settings are needed to augment outcrop CLTZ examples (e.g., Hodgson and Haughton 2004; Bernhardt et al. 2011; Hofstra et al. 2015, 2018; Pemberton et al. 2016; Brooks et al. 2018). However, identifying the CLTZ of an individual depositional system can be difficult in active-margin fans, which are often fed by two or more depositional systems (e.g., Piper and Normark 2001; Ercilla et al. 2008b; Normark et al. 2009b).

The San Gabriel Canyon–Channel system (after Normark et al. 2009b) and the Catalina Basin, offshore southern California, USA, present a unique opportunity to study a relatively small terminal depocenter of a single canyon–channel system crossing a tectonically complex and areally confined region of active faults and inherited structures (Fig. 1) (e.g., Normark et al. 2004; Ryan et al. 2009, 2012). Normark et al. (2004) hypothesized that the Catalina Basin contained a CLTZ as part of the San Gabriel depositional system. Recent high-resolution seafloor and subsurface data collected across the Catalina Basin provide an opportunity to evaluate this hypothesis, characterize an entire CLTZ with a high-resolution dataset, and interpret late Pleistocene and Holocene sedimentation in the Catalina Basin. Specifically, we address the following questions: (1) Is there a CLTZ from the San Gabriel Channel in the Catalina Basin? (2) Is the transition from confined channel to terminal lobes tectonically controlled? (3) Does the CLTZ align with existing conceptual models for spatial distribution of CLTZ depositional and erosional features (e.g., Wynn et al. 2002), including a confined channel, scour field, sediment waves, and lobes? We interpret seafloor and shallow subsurface data in the Catalina Basin and discuss the significance of this CLTZ and its tectonic setting.

REGIONAL BACKGROUND

The Catalina Basin (Fig. 1) is located in the southern California Inner Continental Borderland (ICB), where complex basin and ridge bathymetry developed as the North American–Pacific plate boundary evolved from a subduction zone to a transform margin in the early Tertiary (e.g., Crouch 1981; Vedder 1987). Following early Miocene crustal extension due to the rotation of the Western Transverse Ranges to the north (e.g., Crouch and Suppe 1993; Nicholson et al. 1994; Bohannon and Geist 1998), the ICB experienced transpression starting in late Miocene to early Pliocene time (e.g., Vedder 1987*)*. The ICB is characterized by generally NW-trending offshore faults thought to be Quaternary-active dextral strike-slip components of the broader San Andreas Fault System (e.g., Legg 1991; Legg et al. 2007; Fisher et al. 2009; Ryan et al. 2009) that accommodate approximately 10–15% ($\sim$ 6–8 mm/yr) of North American and Pacific plate relative motion between the shoreline and San Clemente Island (Bennett et al. 1996; DeMets et al. 2010; Platt and Becker 2010). The Catalina Fault and the San Clemente Fault bound the Catalina Basin to the northeast and southwest, respectively, creating an oblong depression, oriented approximately NW–SE between San Clemente Island and Catalina Island (Fig. 1). The southeastern basin contains numerous basement highs, including Emery Knoll and the northern extension of Thirtymile Bank, that separate the Catalina Basin from other ICB basins (e.g., Teng and Gorsline 1989) and may be related to subduction, transtension, volcanism, or other tectonism that preceded development of the major Quaternary-active faults (Legg et al. 2004b).

The Catalina Basin is considered a transitional basin in the Borderland because it receives continent-derived sediment from the San Gabriel Canyon–Channel system in addition to local sediment sources from adjacent islands and platforms (Teng and Gorsline 1989; Normark et al. 2004, 2009b). Two main heads of the San Gabriel Canyon (Fig. 1A) incise the continental shelf 8–18 km from the shoreline and $<$ 2 km from the shelf edge with up to $\sim$ 85 m relief (e.g., Normark et al. 2009a; Dartnell et al. 2015). The Los Angeles and San Gabriel rivers may have transported sediment at rates on the order of 1.2×10^9 tons per year (Warrick and Farnsworth 2009) during sea-level lowstands in channels across the exposed continental shelf to the heads of the San Gabriel Canyon (Sommerfield et al. 2009). Holocene sea-level rise has effectively disconnected supply of terrestrial sediment from the San Gabriel Canyon, leaving the Modern canyon system and outer shelf dominated by hemipelagic accumulation (Alexander and Lee 2009; Sommerfield et al. 2009), which is $<$ 2 m thick along the San Gabriel Channel (Normark et al. 2009b, Ryan et al. 2012). The San Gabriel Canyon heads continue from the shelf edge down the continental slope until $\sim$ 450 m water depth, where they merge to form the San Gabriel Channel (Normark et al. 2004), with relief over 100 m on the continental slope. This channel splits into an eastern arm along Lausen Knoll and a western arm that continues into the Catalina Basin (Fig. 1A). The eastern arm has been interpreted to end down-slope in a depositional lobe with prominent sediment waves on the seafloor, based on earlier seismic-reflection profiles and multibeam bathymetry (Normark et al. 2004, 2009b). The western San Gabriel Channel exhibits erosional benches, a morphologic term for relatively higher, flat areas adjacent to a channel axis or thalweg (as in Maier et al. 2012), until it reaches the Catalina Basin (Teng and Gorsline 1989; Normark et al. 2004, 2009b). Following Teng and Gorsline (1989) and Normark et al. (2004, 2009b), we argue that the San Gabriel Channel fed a fan in the Catalina Basin.

Although the Catalina Basin has been investigated for decades with sampling and subsurface imaging studies (e.g., Emery 1960; Emery and Bray 1962; Moore 1969; Chang and Douglas 1987; Brandsma et al. 1989; Teng and Gorsline 1989; Legg et al. 2004b; Normark et al. 2004), no borehole data or deep-penetration cores have been acquired in the Catalina Basin, and little characterization is available below the uppermost muddy, shallow sediments. Teng and Gorsline (1989) mapped seismic facies in proprietary industry deep-penetration seismic-reflection profiles across the Catalina Basin to interpret upper, middle, and lower submarine fan deposits in the basin and to identify a small fan-shaped accumulation from Catalina Canyon. They were unable to resolve any CLTZ later hypothesized by Normark et al. (2004) because no comprehensive grids of high-resolution data were available in the Catalina Basin that would allow further investigation, before this study.

METHODS

High-resolution seafloor and subsurface data were collected across the Catalina Basin in 2014 and 2016. The University of Washington and U.S. Geological Survey (USGS) acquired multibeam bathymetry and acoustic backscatter data from a hull-mounted Kongsberg EM302 Multibeam Echosounder on the R/V *Thomas G. Thompson* in February 2016. Multibeam bathymetric data were processed and gridded at 10 m resolution (vertical resolution $\sim$ 5 m) and merged with existing multibeam data (Dartnell et al. 2017). Seafloor slope maps and profiles were derived using ArcGIS software. Down-slope profiles are extracted from 10 m grids at 10 m spacing and smoothed over a sliding 50 m window. Seafloor gradient is determined from the change in relief over a lateral distance along these profiles. We combine bathymetry with 15-m resolution acoustic backscatter, a complex signal of seafloor roughness, hardness, and composition, to aid in interpreting near-seafloor deposits (e.g., Gardner et al. 2003). Backscatter data are displayed with ArcGIS software as stretched standard deviations ($n = 1$) using bilinear interpolation.

The USGS acquired high-resolution chirp sub-bottom profiles and multichannel seismic-reflection (MCS) data across the Catalina Basin in November 2014 from the R/V *Robert Gordon Sproul*. Chirp data were acquired with a hull-mounted Knudsen 320B 3.5 kHz digital echosounder. MCS data were acquired initially with a 6 kJ sparker source operated at 5 kJ for the first four profiles (Sproul Lines 1–4), and subsequently with a 700 J mini-sparker source. MCS data were recorded on a 300-m-long, 48-channel digital Geometrics GeoEel streamer with 6.25 m group spacing

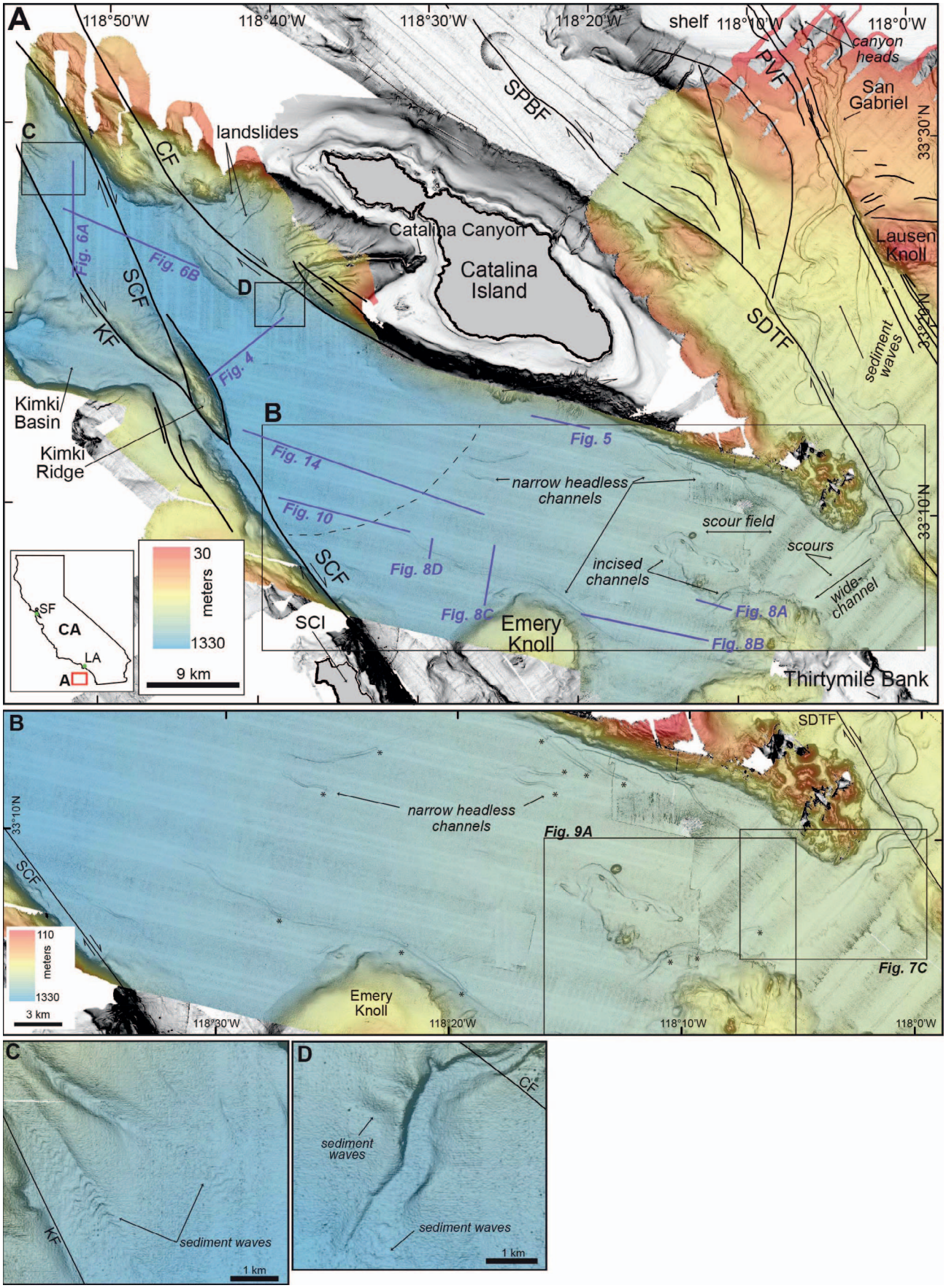

and depth control birds. Additional high-resolution MCS and chirp profiles were collected simultaneously with bathymetry in February 2016 aboard the R/V *Thomas G. Thompson* using a 700 J mini-sparker source and 150-m-long, 24-channel analog Geometrics MicroEel streamer with 6.25 m group spacing, and a hull-mounted Knudsen 3260/320BR 3.5 kHz echosounder, respectively. MCS data were processed to post-stack time migration using SioSeis, Echos, and Seismic Unix software through f-k migration and included deconvolution steps to suppress short-period multiples (e.g., bubble pulses, ghost reflections), resulting in broadband data that greatly increases the vertical resolution (~ 1.5–3 m) of seismic images. Chirp profiles were converted to envelope, and horizons were picked using IHS Kingdom Suite software. Horizons and isochron packages were interpolated using IHS Kingdom Suite inverse distance to a power gridding. A constant time-depth conversion of 1500 m/s is applied to approximate depth and thickness of shallow subsurface units.

RESULTS

Herein, we present the Catalina Basin margins and basin-floor features to evaluate sediment sources to basin fill, relative timing of deposition, and depositional processes. We first describe the steep northern and northwestern basin margins that contain small sediment accumulations of limited lateral extent. We then describe basin-floor features, including channels (considered to be well-defined continuous conduits with measurable incisional or leveed relief), scours (dominantly erosional, enclosed depressions that truncate underlying deposits; after Symons et al. 2016), narrow, apparently disconnected channels (i.e., headless, after Normark 1985; down-dip, and appearing disconnected, from continuous channels), knickpoints (short, steep channel segments between lower-gradient segments; e.g., Heiniö and Davies 2007), and possible small sediment waves (crescentic to sinuous, symmetrical to asymmetrical, upslope-migrating bedforms that can form under turbidity flows as net depositional cyclic steps; e.g., Normark et al. 1980; Wynn et al. 2000a, 2000b; Symons et al. 2016; Covault et al. 2017; Maier et al. 2017). We present interpreted seismic horizons that delineate depositional packages in the shallow subsurface, including lobes (herein defined largely from seismic-reflection profiles as sheet-like units with relatively uniform seismic character, cross-sectional lens shape, and somewhat elongate map-view distribution; e.g., Normark et al. 1979; Mutti and Normark 1987; Wynn et al. 2002; Prélat et al. 2010).

Catalina Basin Margins

The Catalina Basin (Figs. 1–3) has steep margins along San Clemente Island and Catalina Island. The steep northern basin margin along Catalina Island includes (1) a western segment with Catalina Canyon (after Emery 1960; Teng and Gorsline 1989) and sediment waves, adjacent small incised channels, and submarine landslides, and (2) an eastern segment where small sediment accumulations (< 1 km width), bright elongate areas in backscatter, and few small channels (~ 100–200 m width) are observed at the base of the steep Catalina Escarpment near the eastern tip of Catalina Island (Figs. 1, 2). A deposit of limited lateral extent and radial fan shape topped by sediment waves is imaged at the mouth of Catalina Canyon (e.g., Figs. 2B, 4). Along the eastern segment south of Catalina Island, the base of escarpment accumulations thin to the NW and SE along the margin and are incised by channels (Figs. 1, 5). The northwestern margin of the Catalina Basin contains at least three submarine channels (~ 200 m–1 km width; up to ~ 20 m relief) that are oriented approximately south-southeast, contain sediment waves, and appear to end at the base of slope in two lobes that do not extend to basin margins or the San Clemente Fault (Figs. 1C, 6).

Catalina Basin Floor

The high-resolution bathymetry and subsurface profiles show that the main portion of the Catalina Basin narrows to the northwest and contains an adjacent structurally isolated subbasin west of the San Clemente Fault, distinguished from the Catalina Basin (Kimki Basin in Fig. 1). The Catalina Basin floor morphology and subsurface character changes from east to northwest. Overall, the seafloor gradually flattens from the San Gabriel Channel into the Catalina Basin but contains numerous local gradient breaks (Fig. 3). The San Gabriel Channel enters the easternmost Catalina Basin as a confined single channel with knickpoints up-dip from the San Diego Trough Fault (Figs. 1, 3B) and benches at a narrow (~ 3.5 km) opening flanked by two basement highs (Figs. 1, 3E). Where the channel continues past the basement highs, it rapidly widens and decreases in relief (Fig. 3E–G). Channel width increases from ~ 600 m wide in the San Gabriel Channel axis to ~ 2.4 km wide in the basin, accompanied by a decrease in channel relief from ~ 80 m to < 10 m, across ~ 5 km lateral distance before the northern channel margin becomes unresolved (Fig. 7). Aspect ratio (channel width divided by channel relief; AR; e.g., Carvajal et al. 2017) changes from up to ~ 25–50 across the basin opening and San Gabriel Channel (Fig. 3E), to ~ 67 to 800 in the basin. As the channel widens, scours (~ 100–300 m length, up to ~ 500 m width, and elongate approximately perpendicular to the channel paleoflow) appear at the channel margins (Figs. 3G, H, 7) where seafloor gradient along the channel increases slightly from < 0.1° to ~ 0.2° (Fig. 3B inset).

Farther into the basin, narrow (~ 100–200 m width; ~ 10–15 m relief) channels appear not to be directly connected to the wide channel. These narrow channels occur across the shallow to mid-basin, particularly adjacent to faults and basement highs, and contain abrupt increases in the channel-floor depth over short distances, termed knickpoints (e.g., Heiniö and Davies 2007; Wynn et al. 2007). These channels increase in width and AR (from ~ 30 to 40) down basin until they disappear (Figs. 1D, 8C, D). The narrow channels truncate adjacent moderate- to high-amplitude shallow reflections that appear less continuous down-slope (Fig. 8). Where shallow channel fill is resolved, parallel and continuous moderate- to high-amplitude reflections are imaged (Fig. 8A, C).

Between two of the narrow channels, a small field (~ 30 km^2) of relatively small (mostly ~ 100 m length, ~ 200 m width, up to ~ 10 m relief), crescent-shaped scours is imaged, up-dip from basement highs (Fig. 9). The scour field, scour-headed channel, and apparently disconnected channels are incised between structural blocks and create abrupt, localized increases in seafloor gradient across the northern extension of Thirtymile Bank (Fig. 3D). A large scour (375 m width, 275 m length, ~ 30 m relief) transitions into a wide, poorly confined channel (up to 1 km width, < 10 m relief, AR > 100) that passes between two basement highs and appears to contain at least one knickpoint. Channels generally display greater relief (~ 10–25 m) adjacent to basement highs. Like the narrow channels, scours and the scour-headed channel truncate underlying reflections, and in some locations, appear partially filled by continuous, moderate- to high-amplitude reflections (Fig. 9).

Compared to the northwestern part of the basin, the shallower, eastern part of Catalina Basin has a slightly higher gradient (~ 0.4°) that continues to the distal extent of channels at approximately 1230–1290 m water depth

←

FIG. 1.—Color-contoured slope-shaded multibeam bathymetry gridded at 10 meters. **A)** The Catalina Basin and the San Gabriel Canyon–Channel depositional system. Dashed line in the Catalina Basin indicates approximate extent of channels resolved on the seafloor. **B)** Shallow to mid-Catalina Basin. Stars indicate knickpoints. Black lines are faults: SCF, San Clemente Fault Zone; KF, Kimki Fault; CF, Catalina Fault Zone; SDTF, San Diego Trough Fault Zone; SPBF, San Pedro Basin Fault Zone; PVF, Palos Verdes Fault Zone. SCI, San Clemente Island. Sediment waves in **C)** Northwest channels and **D)** Catalina Canyon.

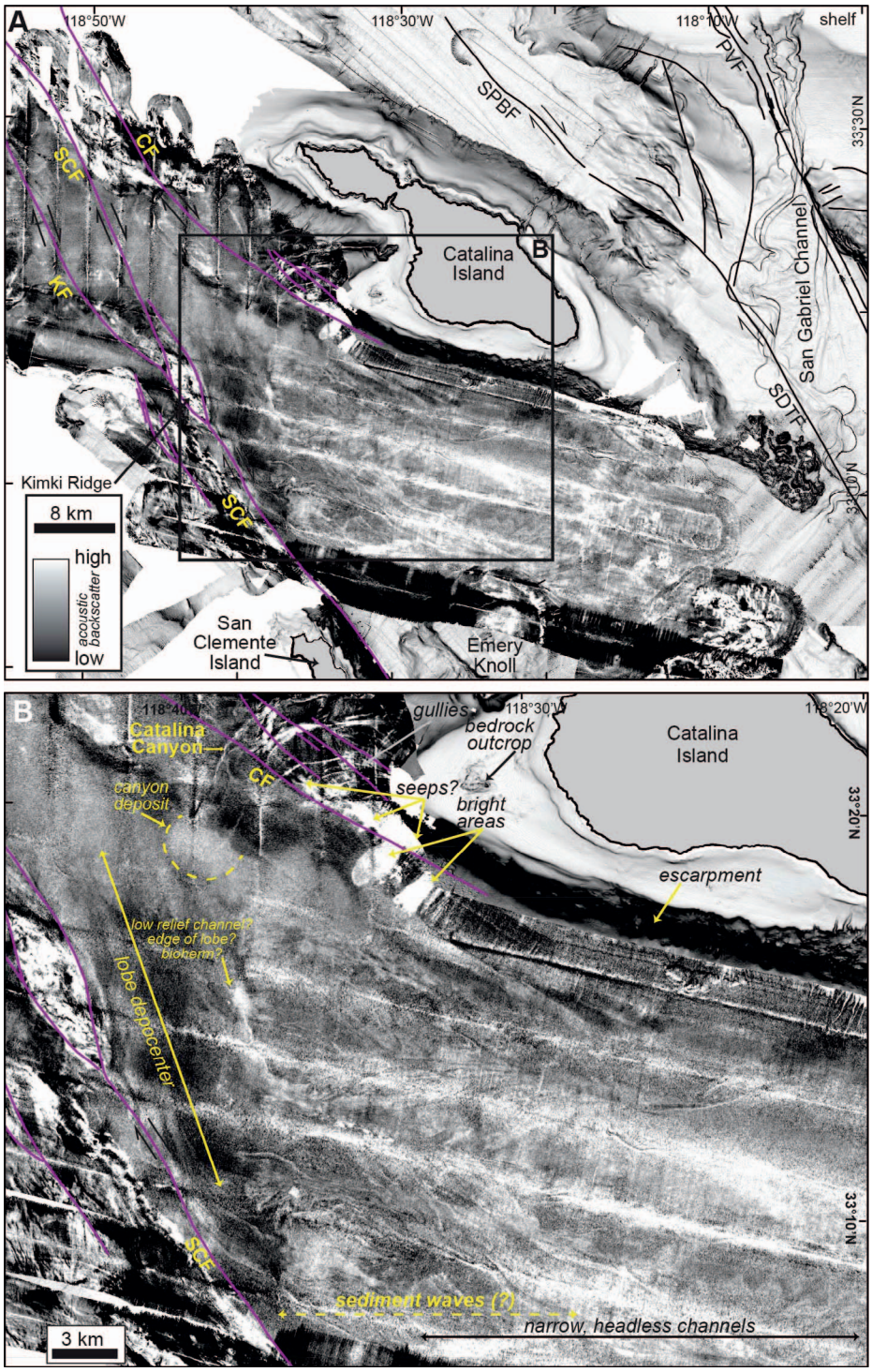

FIG. 2.—Acoustic backscatter gridded at 15 meters. Lighter areas are high backscatter, and darker areas are low backscatter. Faults as in Figure 1. Backscatter shown on slope-shaded multibeam bathymetry. **A)** Catalina Basin survey. **B)** Enlarged mid-basin.

in the mid-basin (Figs. 1–3). Seafloor profiles approximately perpendicular to paleoflow show a rapid cross-sectional flattening of the seafloor and decrease in channel relief into the basin (Fig. 3E, F). The basin cross-sectional relief, although dwarfed by structural relief at the basin margins, is consistently sloped (up to $\sim 0.3°$) towards the southern basin margin or away from the mid-basin (Fig. 3G–K). Beyond where narrow, possibly disconnected channels are clearly resolved, an area of complex high and low backscatter persists for an additional $\sim$ 8–15 km (Fig. 2), wherein overall gradient transitions from $\sim 0.2°$ (locally up to $\sim 0.4°$) to $< 0.1°$ in the deeper basin (Fig. 3D). Seismic reflections across this area of slightly increased seafloor gradient appear wavy with subtle accumulations on the upper limbs of dipping reflections, indicative of up-slope migration common in sediment waves (Fig. 10).

Shallow Subsurface Horizons

In general, chirp subsurface reflections increase in continuity and depth of imaging from the shallower to deeper parts of the Catalina Basin. Three

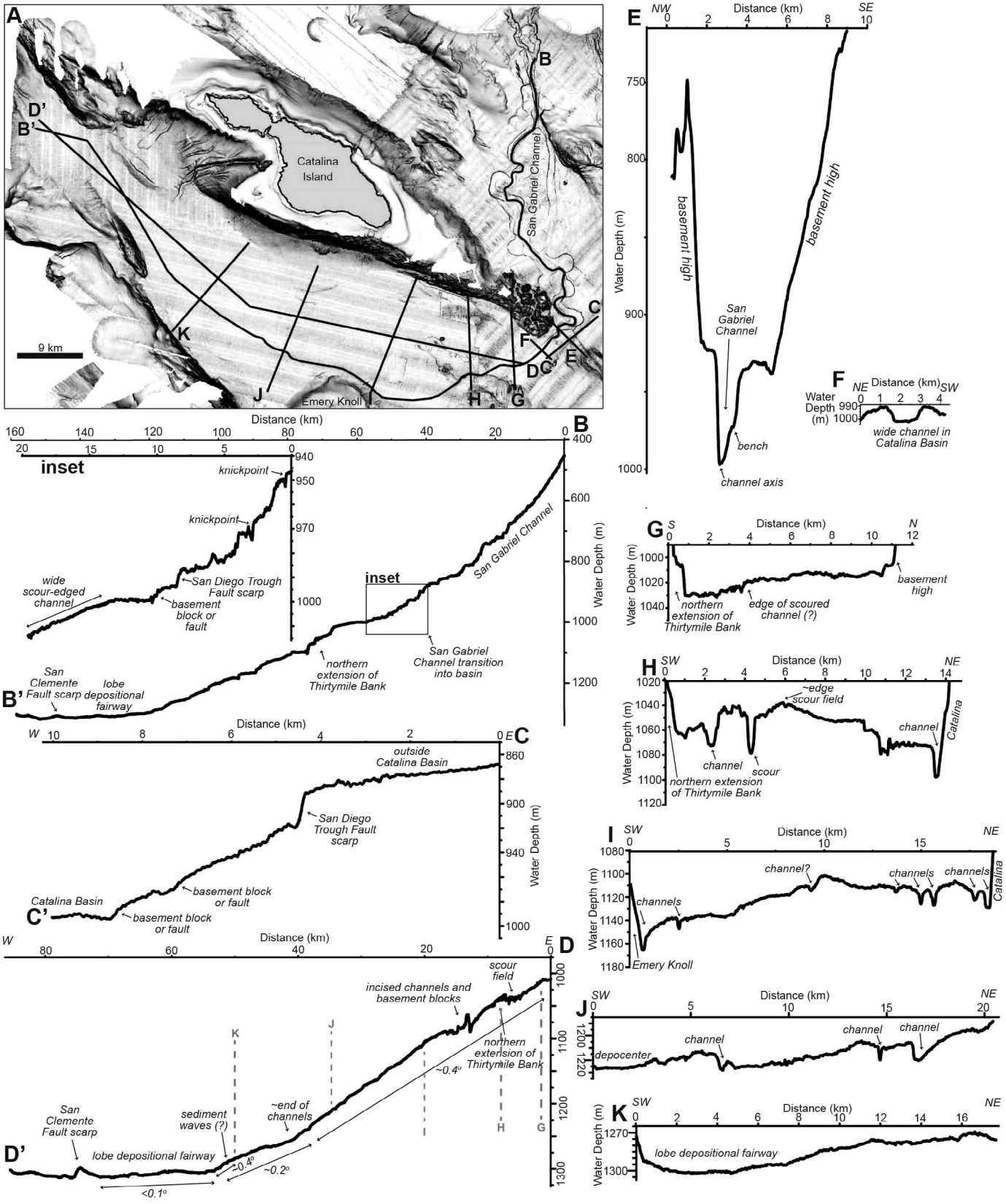

FIG. 3.—Seafloor profiles. **A)** Seafloor profile locations on slope-shaded multibeam bathymetry (shown in greater detail in Fig. 1). **B)** San Gabriel depositional system (VE ~ 100×). Inset shows enlarged (VE ~ 200×) part where the confined channel enters the basin. **C)** Profile into the Catalina Basin from outside the channel (VE ~ 25×). **D)** Catalina Basin (VE ~ 100×). Dashed lines indicate intersections with cross-basin profiles G through K). **E–K)** Cross-sections from shallow (upper) to deep (lower) in the Catalina Basin shown at the same scale (VE ~ 50×).

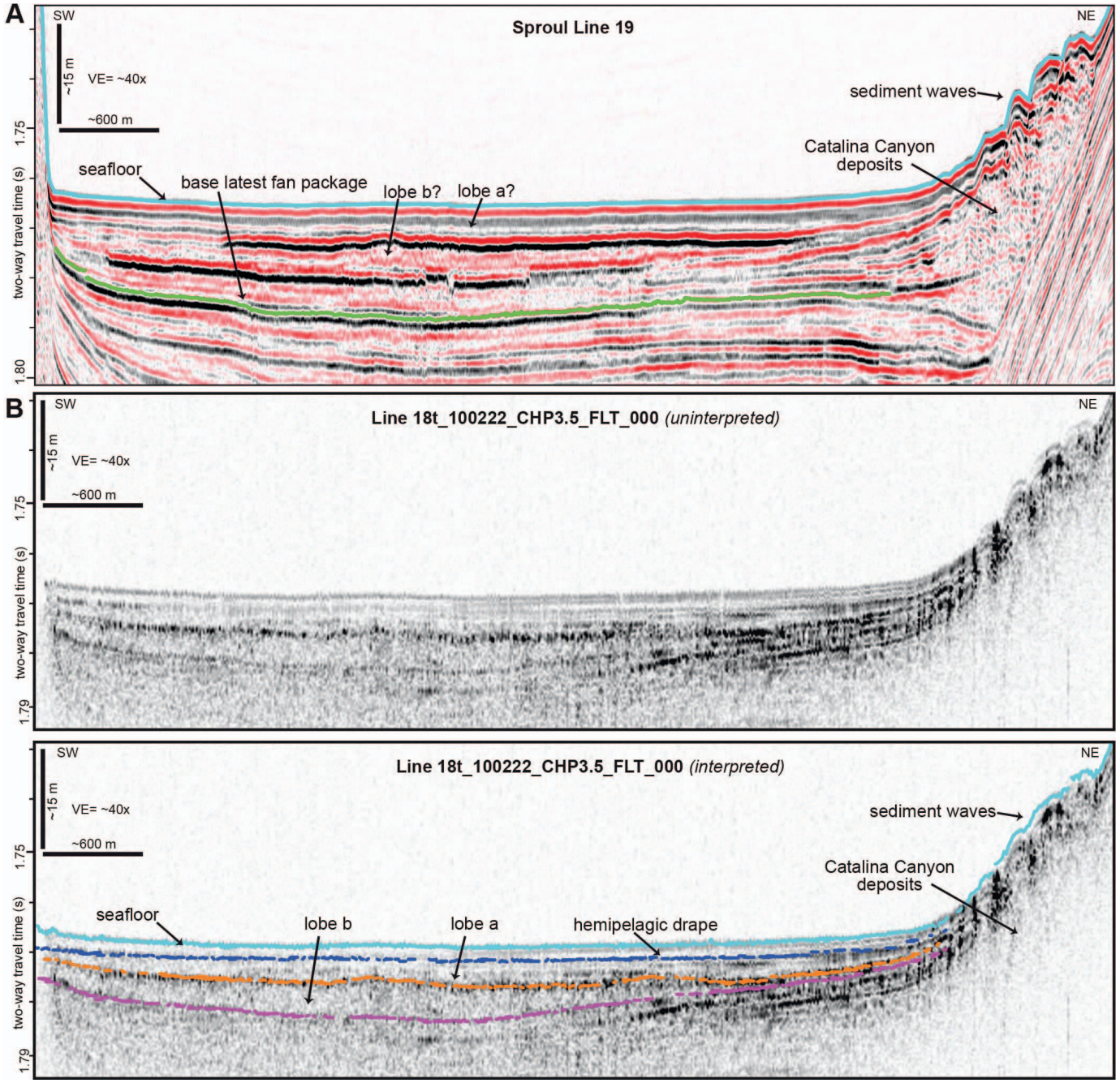

FIG. 4.—Lobe deposits in the Catalina Basin and Catalina Canyon deposits. Lobes onlap deposits from Catalina Canyon that are limited to a base of slope accumulation. See Figure 1A for profile location. **A)** Multichannel profile. **B)** Simultaneously collected chirp profile shown as uninterpreted (above) and interpreted (below).

packages are mapped from horizons correlated between chirp profiles and referred to as (1) base of transparent drape layer (dark blue), (2) base of lobe a (orange), and (3) base of lobe b (purple) (Figs. 4, 10). Throughout the basin, chirp sub-bottom profiles image an acoustically transparent layer, with few, discontinuous internal reflections immediately below the seafloor, that drapes underlying, higher-amplitude reflections (e.g., Figs. 4, 10). The drape layer is $\sim$ 1.5 m thick across most of the basin, but thins slightly adjacent to Catalina Island and thickens slightly in the distal basin (Fig. 11).

In the deeper basin beneath the transparent drape layer, sheet-like layers with largely uniform diffuse reflectivity, and cross-sectional lens shape are termed lobes a and b (Figs. 4, 10). Lobe a overlies lobe b and appears to locally show a very weak degree of compensational stacking (Fig. 4). Both lobes a and b onlap basin margins, Catalina Canyon deposits, and basement highs. Both lobes appear to emanate from the mid-basin and do not appear to extend to the San Clemente Fault in the northwestern basin (Fig. 6). Base surfaces of both lobes dip down-basin (i.e., deeper to the northwest) at $< 0.1°$ gradient (Fig. 12A, C). Lobes a and b contain a depositional fairway or thickness trend oriented parallel to the down-basin trend, generally southeast to northwest and skewed to the southwest (Fig. 12C, D).

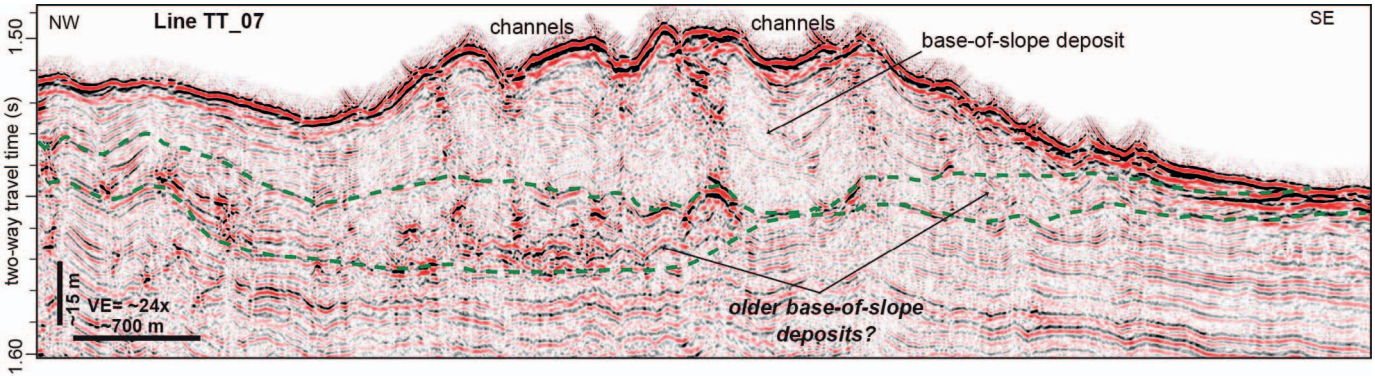

FIG. 5.—Multichannel seismic-reflection profile across base of slope deposits adjacent to southern Catalina Island. See Figure 1A for profile location.

A shallow horizon MCS-a is mapped in the MCS data as a lower bounding reflection of the shallow subsurface unit related to seafloor morphologies and including lobes a and b (Fig. 13; green horizon in Figs. 4, 7–9). This unit, between MCS-a and the seafloor, is termed the latest fan package. It contains depocenters along the southern basin margin that occur adjacent to and separated by fault and ridge structures (Figs. 8B, 13–14).

DISCUSSION

Late Pleistocene and Holocene Sedimentation in the Catalina Basin

We interpret the acoustically transparent drape layer (e.g., Figs. 10, 11) as dominantly a muddy hemipelagic drape, similar to previous high-resolution seismic-reflection studies offshore California (e.g., O'Connell and Normark 1986; Normark et al. 1998; Maier et al. 2011, 2013; Ryan et al. 2012). This interpretation is further supported by previous coring of the upper 1–4 m of sediments in the Catalina Basin that sampled mostly fine-grained muddy sediments, which may be of late Pleistocene and Holocene age (Emery and Bray 1962; Gaal 1966; Schwalbach and Gorsline 1985; Shaw and Johns 1986; Chang and Douglas 1987; Brandsma et al. 1989). Hemipelagic drape is $\sim$ 1.3–1.6 m thick adjacent to the San Gabriel Channel, with a basal age of $\sim$ 12–15 ka (Normark et al. 2009a, 2000b; Ryan et al. 2012). Rates of hemipelagic sedimentation for the eastern Catalina Basin are likely similar to those of the distal San Gabriel Channel ($\sim$ 10 cm/kyr). Thus, the base of the acoustically transparent hemipelagic drape unit in most of the Catalina Basin is likely $\sim$ 15 ka. The consistent presence of the latest Pleistocene and Holocene hemipelagic drape across the Catalina Basin suggests that the basin received minimal terrestrially derived sediment during sea-level rise following the Last Glacial Maximum (LGM) (e.g., Lambeck and Chappell 2001). Thus, the channels, scours, and other features imaged on the basin floor (Figs. 1, 2) are inferred to be of late Pleistocene age, at the youngest.

Seafloor features and reflections between the hemipelagic drape and the MCS-a horizon are interpreted to include at least part of LGM sea-level-lowstand sedimentation in Catalina Basin and be dominated by sediment-density-flow deposits sourced from the San Gabriel Channel. Subsurface profiles show that locally sourced sediments accumulate with limited lateral extents (< 25 km^2) (Figs. 2, 4–6). Lobes a and b onlap the Catalina Canyon deposits (Fig. 4) and dip down-basin (Fig. 12); thus, they are interpreted as a result of flows sourced from the San Gabriel Channel, as opposed to local sources. Furthermore, the potential volume of sediment available to the Catalina Basin from adjacent islands and platforms is dwarfed by the potential sediment contribution of the Los Angeles and San Gabriel rivers during sea-level lowstands (e.g., Sommerfield et al. 2009; Warrick and Farnsworth 2009).

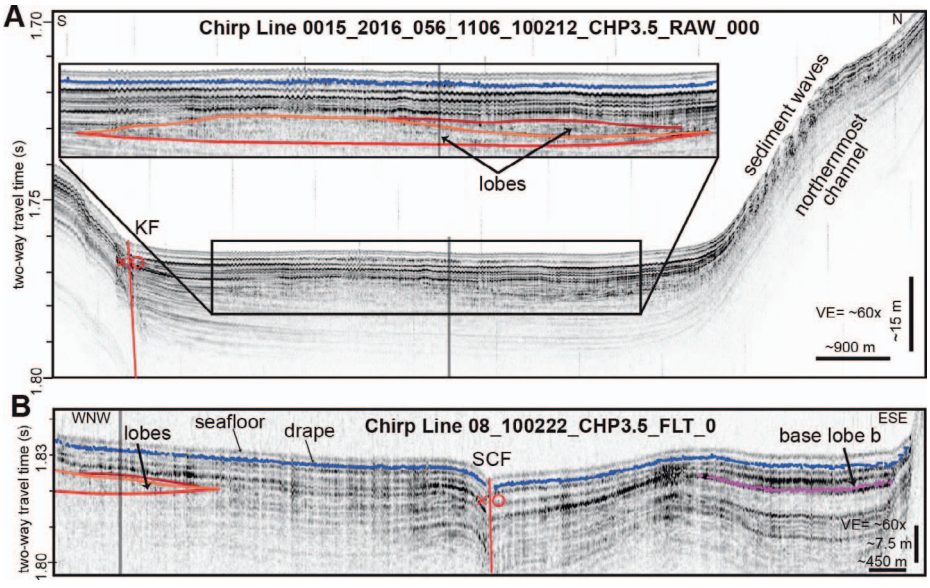

FIG. 6.—Northwest channels and lobes. See Figure 1A for profile locations. Gray lines represent profile intersections. **A)** Chirp profile across the northwestern Catalina Basin shows the stacking of lobes that do not reach the Kimki Fault (KF). **B)** An obliquely oriented chirp profile shows that the lobe deposits originate from the northwest channels, end before reaching the San Clemente Fault (SCF), and do not overlap in extent with lobe b.

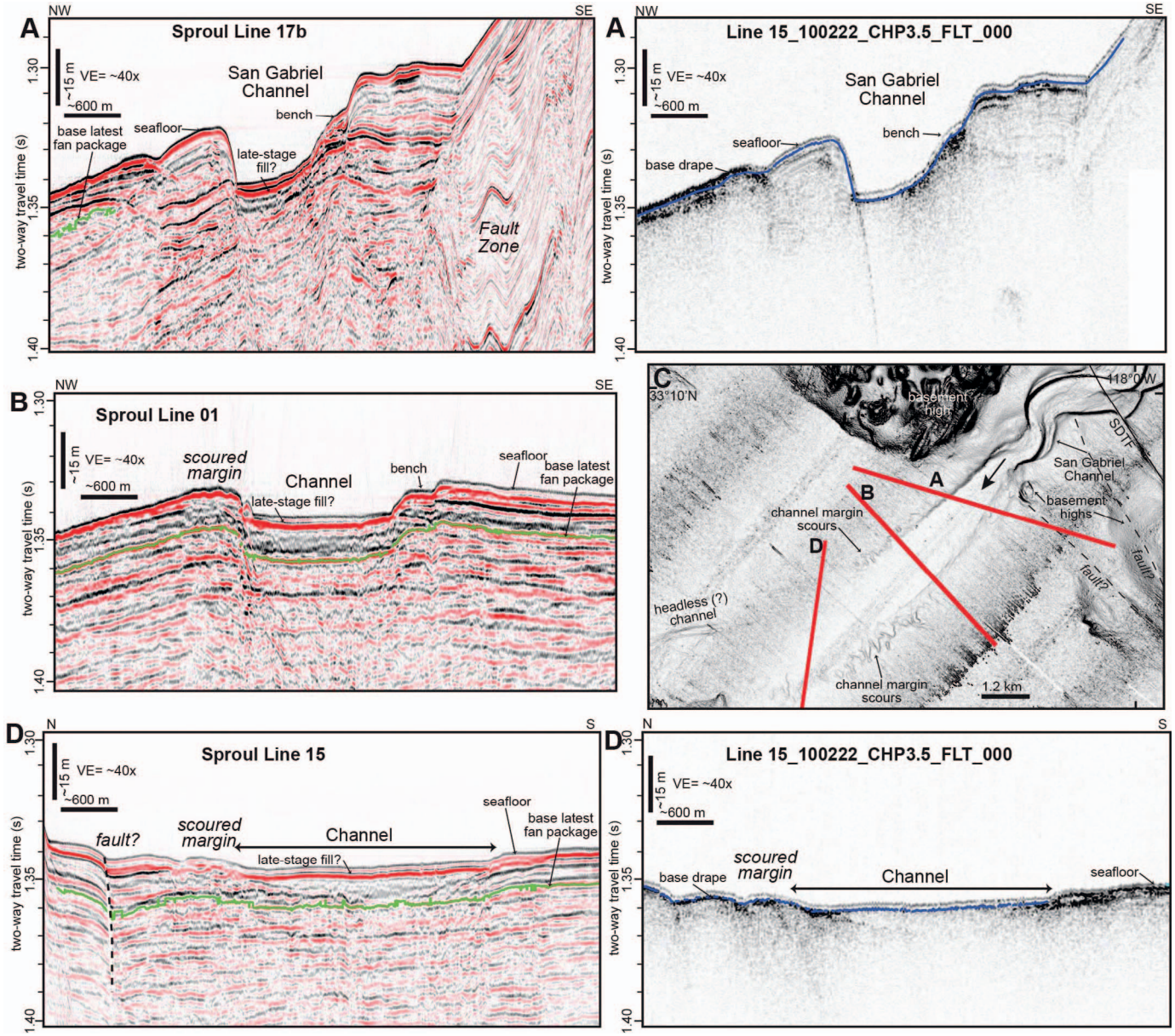

FIG. 7.—Channel entering the Catalina Basin. **A)** Multichannel seismic-reflection (MCS) profile (left) and simultaneously collected chirp profile (right) show an oblique cross section of the channel adjacent to the basement highs. **B)** MCS profile shows a cross section of the channel farther into the Catalina Basin where it has widened and decreased in relief. **C)** Slope-shaded multibeam bathymetry gridded at 10 meters showing profile locations. Arrow indicates general paleoflow direction. SDTF: San Diego Trough Fault. **D)** MCS profile (left) and simultaneously collected chirp profile (right) show an oblique cross section of the wide channel where it has developed scoured edges.

Channel–Lobe Transition Zone Interpretations

We interpret that seafloor and shallow subsurface features imaged in the Catalina Basin comprise a channel–lobe transition zone (CLTZ). We interpret seismic-reflection units termed lobes a and b to be terminal lobes fed from the San Gabriel Channel > 50 km away from where it appears to lose confinement. We acknowledge that we have limited ability to resolve small, low-relief channels and other features with less than a few meters relief in our data (10 m bathymetric grid and seismic-reflection profiles with ~ 1.5–3 m vertical resolution). However, the scouring at wide channel margins and scour field are similar to higher-resolution (1 m bathymetry) data from the Navy Fan (Carvajal et al. 2017). The San Gabriel Channel increases in width more dramatically than the Navy Fan Channel (maximum width ~ 2.4 v. 1 km) with an apparently higher increase in aspect ratio (up to ~ 150/km v. ~ 18/km). Our data demonstrate that seafloor morphology and shallow stratigraphy differ beyond the wide channel, and these down-basin transitions in relief and confinement would have triggered changes in flow dynamics. The wide channel, scours, narrow apparently disconnected channels with knickpoints, and possible sediment waves described herein cumulatively signify a region of complex erosion and deposition characteristic of a channel–lobe transition zone (e.g., Mutti and Normark 1987; Wynn et al. 2002; Postma et al. 2016; Carvajal et al. 2017).

Large sediment waves (hundreds of meters to kilometers in wavelength; 10 m to hundreds of meters wave height) are common features along the Catalina Basin margins (Fig. 1B), San Gabriel Canyon–Channel system (Fig. 1A) (Normark et al. 2004, 2009b), and other CLTZs and deep-sea

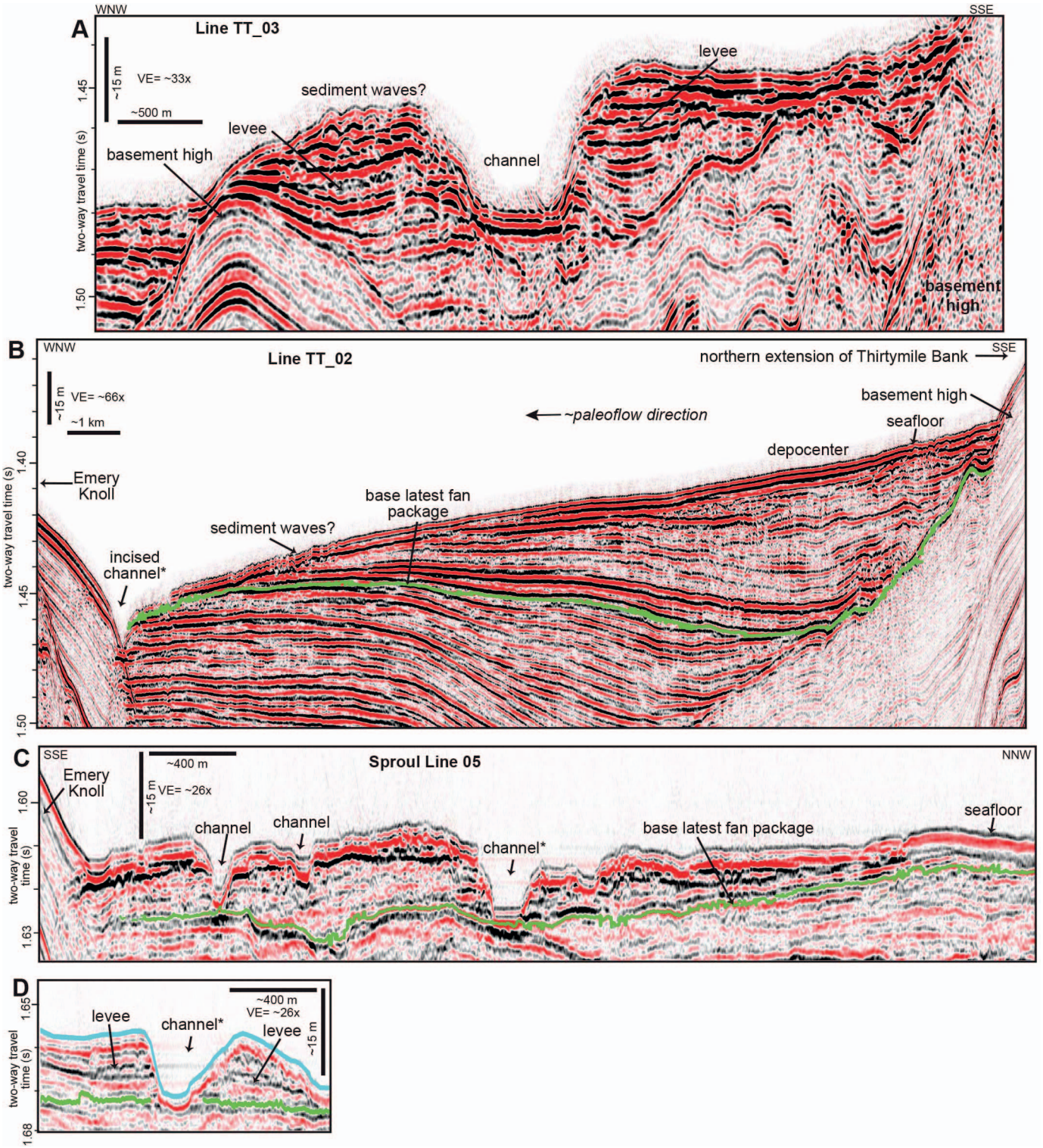

FIG. 8.—Narrow, apparently disconnected channels (i.e., headless; Normark 1985) with knickpoints in multichannel seismic-reflection profiles. See Figure 1A for profile locations. **A)** Line TT_03 shows a channel down-dip from where it crosses a basement high. **B)** Line TT_02 shows a depocenter between two basement highs (right) and a narrow channel incised adjacent to Emery Knoll (left). **C)** Channels on the seafloor that appear contained above the MCS-a horizon and appear disconnected from the San Gabriel Channel. **D)** The down-dip extension of channel (*), where it has increased in width and developed levees.

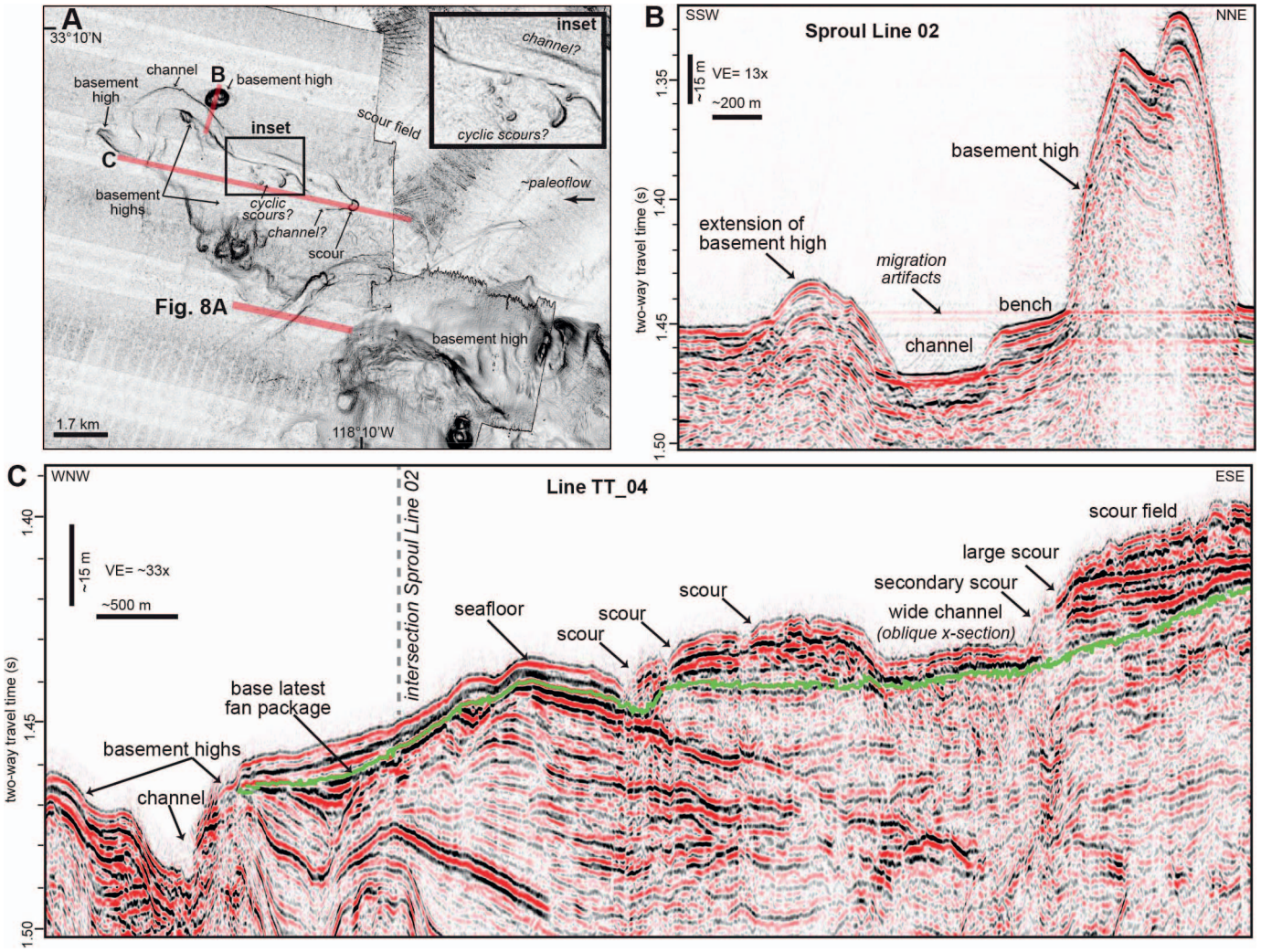

FIG. 9.—Scour-headed incised channel and scour field. **A)** Slope-shaded multibeam bathymetry gridded at 10 meters showing profile locations. **B)** Multichannel seismic-reflection (MCS) profile Sproul Line 02 shows the scour-headed channel incised and confined between two basement highs. **C)** MCS profile TT_04 shows an oblique cross section of the initial scour and wide, low-relief channel (right) and a cross section of the more distal part of the same channel where it is again incised and confined between basement highs (left).

settings (e.g., Normark et al. 1980 and references therein; Wynn et al. 2000a, 2000b and references therein; Wynn and Stow 2002; Bonnel et al. 2005; Kuang et al. 2014, and many others). However, sediment waves are conspicuously absent in multibeam bathymetry across the Catalina Basin CLTZ. It is possible that sediment waves were not formed, owing to apparent low gradients between the narrow channels and mapped lobe deposits (Fig. 3); however, small-scale sediment waves may be imaged in the CLTZ where seafloor gradients increase slightly (up to 0.4°) immediately up-dip from mapped lobe deposits (Figs. 3D, 10). We interpret that these up-slope-migrating bedforms (Fig. 10) are sediment waves formed in sediment density flows, as opposed to creep-related wave features (after Symons et al. 2016). These sediment waves (Fig. 10) are an order of magnitude smaller than most other modern seafloor CLTZ examples (e.g., Symons et al. 2016; Covault et al. 2017 and references therein; Hofstra et al. 2018); they are of scale similar to that of fine-grained sediment waves documented from the unconfined continental slope adjacent to the San Gabriel Canyon (Maier et al. 2017) and to those imaged in the Navy Fan CLTZ (Carvajal et al. 2017).

Influence of Inherited Structure and Active Tectonics

Depositional processes in the CLTZ are mainly influenced at multiple scales by the tectonic setting of the ICB, which is a conglomeration of inherited basement structures from preceding phases of tectonism (e.g., Crouch 1981; Vedder 1987; Crouch and Suppe 1993; Bohannon and Geist 1998; ten Brink et al. 2000), as well as Quaternary-active strike-slip and transpressional components of the San Andreas Fault System (e.g., Legg 1991; Legg et al. 2007, 2015). Similar to other ICB fans (Buffington 1964; Shepard et al. 1969; Graham and Bachman 1983; Piper and Normark 2001; Covault and Romans 2009) and deep-sea deposition in other tectonically active settings (e.g., Remacha et al. 2005; Ercilla et al. 2008a), the shapes and orientations of the San Gabriel Fan, CLTZ, individual lobe deposits, and flow paths (e.g., Fig. 15) are determined by the structurally controlled basin geometry. Tectonic structure in and around Catalina Basin provides large-scale confinement to the distal extent of the San Gabriel depositional system. Although the San Gabriel channel enters the basin oriented to the southwest, flows are effectively turned by structural relief along the southern basin margin such that, by the mid- to distal CLTZ,

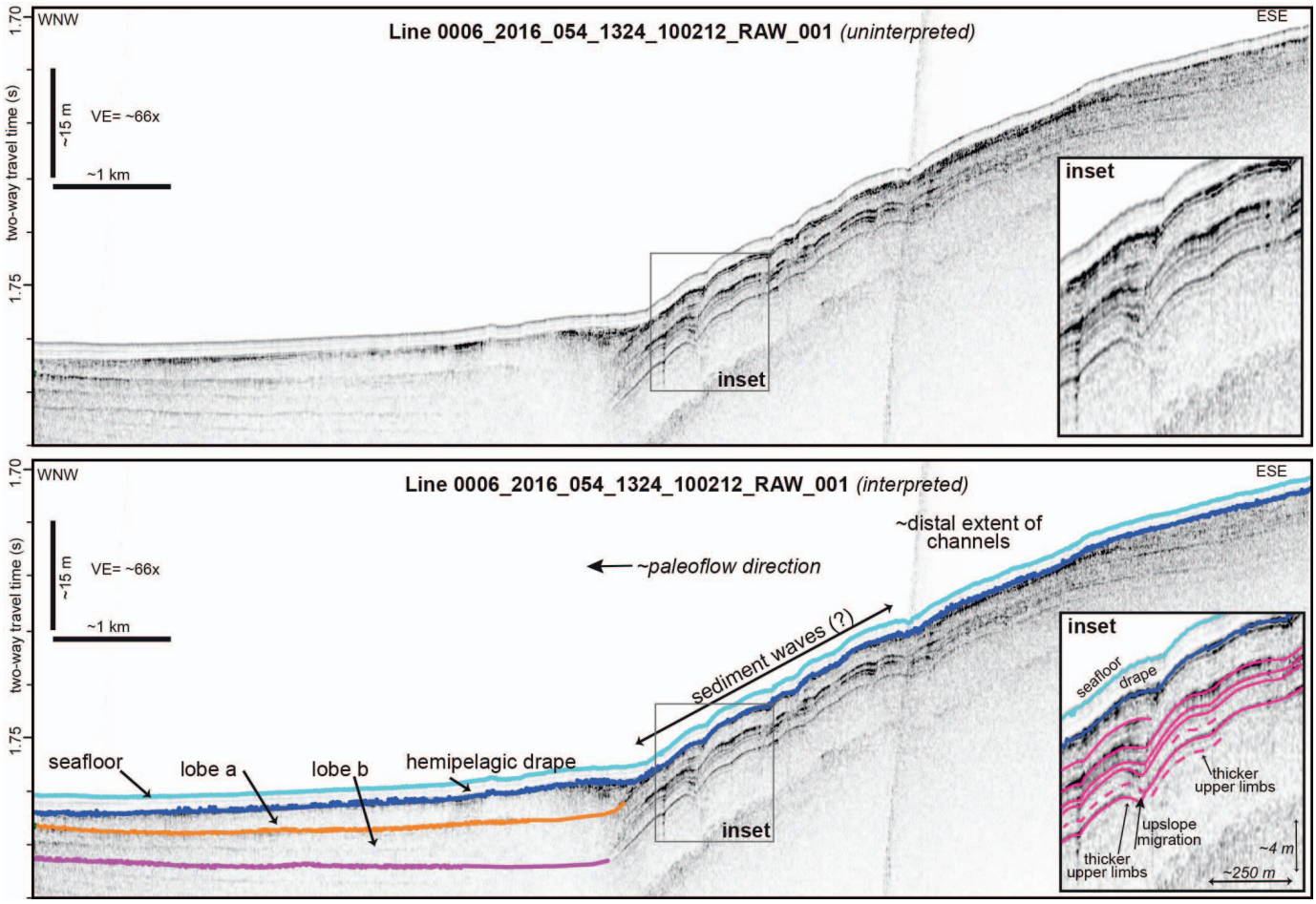

FIG. 10.—Chirp profile across the mid-Catalina Basin (see Fig. 1A). Small-scale sediment waves on the order of ~ 200–300 m wavelength and ~ 2–4 m wave height may be imaged in this profile (inset) but remain below the resolution of multibeam bathymetric data. Sediment waves are interpreted between the distal extent of the narrow, apparently disconnected channels and lobes a and b.

paleoflow was headed towards the northwest. Steep relief at the basin margins, persistent down-basin gradients (Fig. 3), and increasing confinement from the narrowing basin (Fig. 15) are factors that influence flow directions and funnel fan sediments to the northwest in elongate lobe packages that onlap and are contained by basement highs (e.g., Lomas and Joseph 2004; Remacha et al. 2005; Liu et al. 2018). Thick successions of stacked lobe deposits are ponded, with map-view distribution and thickness trends determined by basin shape (Fig. 12) (e.g., Gervais et al. 2006; Prélat et al. 2010). This large-scale depositional architecture differs from fans and CLTZs in larger basins, where terminal deep-marine deposits are characterized by channel avulsion, elongate and rounded lobe shape, and more radial overall fan shape (e.g., Babonneau et al. 2002; Fildani and Normark 2004; Klaucke et al. 2004; Maslin et al. 2006; Jegou et al. 2008; Prélat et al. 2010; Ortiz-Karpf et al. 2015; Picot et al. 2016).

Additionally, inherited structures and cross-basin gradients lead to localized depocenters in the San Gabriel CLTZ, segmenting and stacking late Pleistocene fan deposits (Fig. 13) and older basin fill (Fig. 14). Depocenters in the CLTZ (Fig. 13) appear structurally controlled, wherein sediment sourced from the San Gabriel Channel filled existing lows between structural basement blocks. Stratigraphy of the depocenters may contain sedimentation patterns similar to mini-basins in other settings dominated by vertical fault motion or salt tectonics (e.g., Prather et al. 1998; Grecula et al. 2003; Smith 2004). Fill-and-spill concepts and

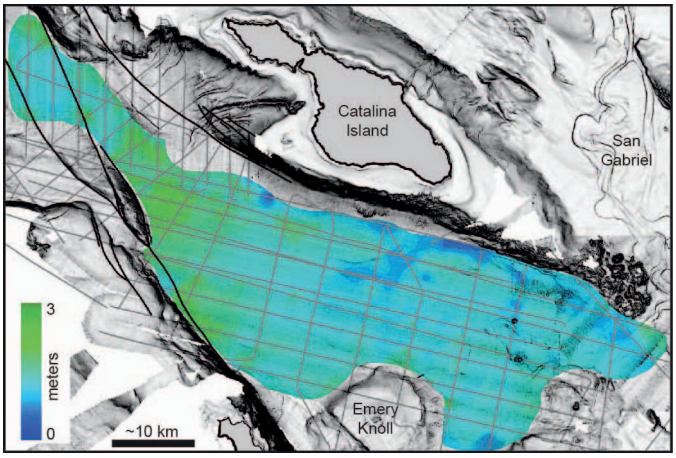

FIG. 11.—Interpolated isochore map of the acoustically transparent drape layer. The drape has similar thickness across the Catalina Basin, with a slight increase in thickness to the northwest. Gray lines show distribution of chirp profiles from which the drape layer was mapped and interpolated. Black lines are faults as in Figure 1.

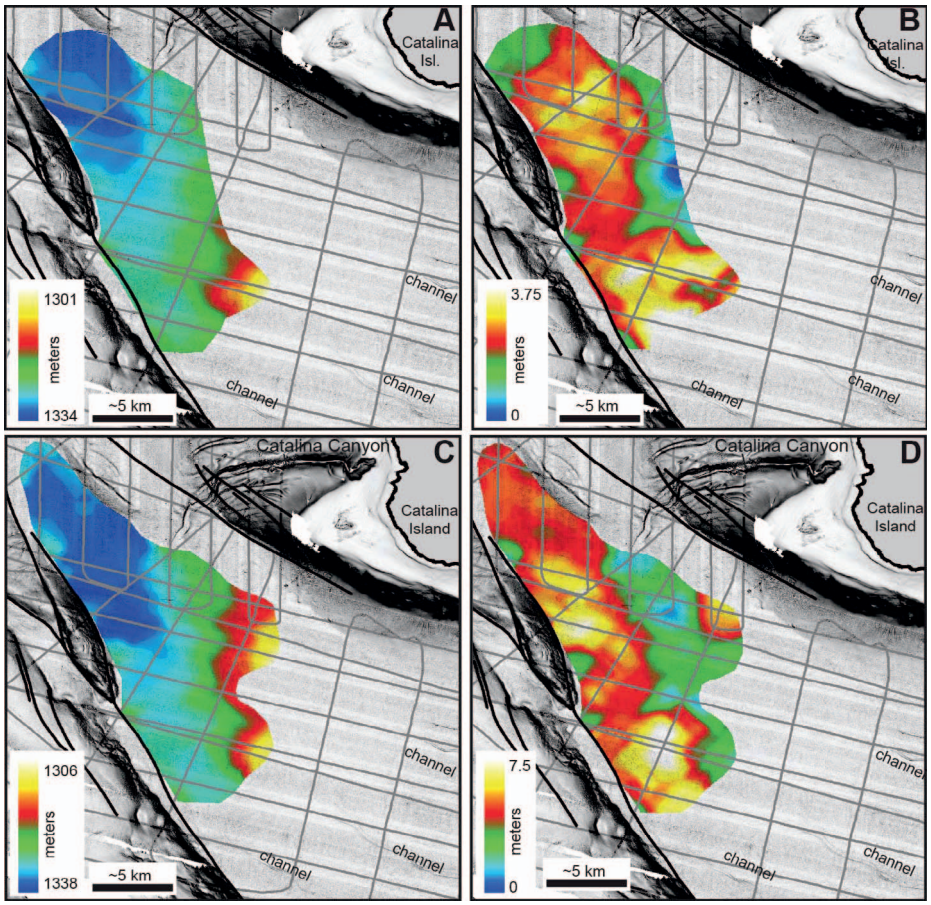

FIG. 12.—Lobes a and b in the Catalina Basin. Lines as in Figure 11. **A)** Interpolated base of the shallowest resolved lobe deposit (lobe a). **B)** Interpolated isochore of lobe a. **C)** Interpolated base of the underlying lobe deposit (lobe b). **D)** Interpolated isochore of lobe b.

sedimentation patterns developed from these settings (e.g., Prather et al. 1998; Marini et al. 2016) may be applicable to deeper records in the Catalina Basin, wherein proximal depocenters in the eastern part of the basin must have ponded sediments, at least partially, before San Gabriel Channel sediment flows could bypass to fill the deeper Catalina Basin.

Tectonic setting also exerts principal influence at a smaller scale by controlling CLTZ depositional architecture and interpreted flow processes. Unlike other channels that are able to avulse (i.e., change location over time) (e.g., see reviews in McHargue et al. 2011; Sylvester et al. 2011), the San Gabriel channel location is locked in the narrow basin opening between two basement highs (e.g., Fig. 3). This tectonic restriction maintains a consistent sediment input location to the basin, and triggers channel incision and creation of benches instead of avulsion. Likewise, basement highs confined flows and sustained a consistent location of rapid decrease in confinement and flow expansion into the basin.

Inherited basement highs and buried structures in the Catalina Basin influence seafloor gradients, which controlled varying morphologies throughout the CLTZ. The northern extension of Thirtymile Bank created breaks in seafloor gradient that may have triggered scouring at the channel margins and formation of the scour field, similar to the influence of buried structures on cyclic scour formation in the San Mateo Channel (Covault et al. 2014). The scour field may contain cyclic scours—a fundamental morphodynamic feature of deep-water depositional systems and CLTZs, forming upstream-migrating, net erosional steps bounded by hydraulic jumps related to underlying structural or depositional relief (e.g., Covault et al. 2014, 2017; Hofstra et al. 2015; Dorrell et al. 2016; Carvajal et al. 2017). Trains of scours may have merged over time in combination with knickpoint migration to form the scour-headed channel (e.g., Fildani et al. 2006, 2013; Maier et al. 2011, 2013). Basement highs, such as Emery Knoll and Catalina Island, create seafloor gradients sloped to the basin margins (Fig. 3G–K), leading to narrow, apparently disconnected channels at the basin margins, where flows moving away from the central-basin structural high appear to have banked against the structural relief and

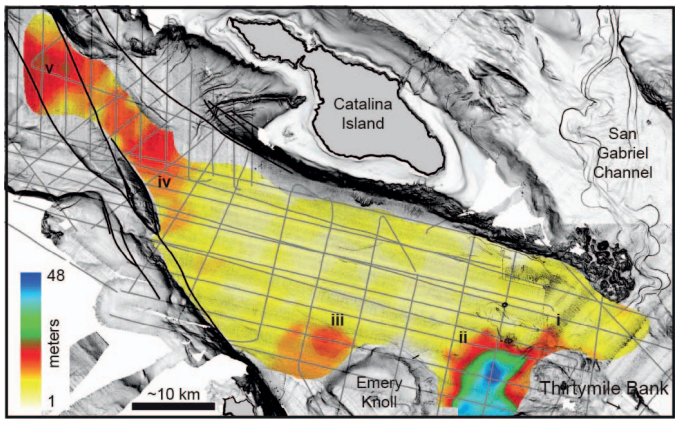

FIG. 13.—Interpolated isochore map above horizon MCS-a. Depocenters in this package occur (i) north of Thirtymile Bank, (ii) between the northern extension of Thirtymile Bank and Emery Knoll, (iii) between Emery Knoll and San Clemente Island, (iv) in the distal basin where lobes a and b are mapped, and (v) adjacent to the northwest channels. Gray lines show the distribution of multichannel seismic-reflection profiles from which the MCS-a horizon was mapped. Black lines are faults as in Figure 1.

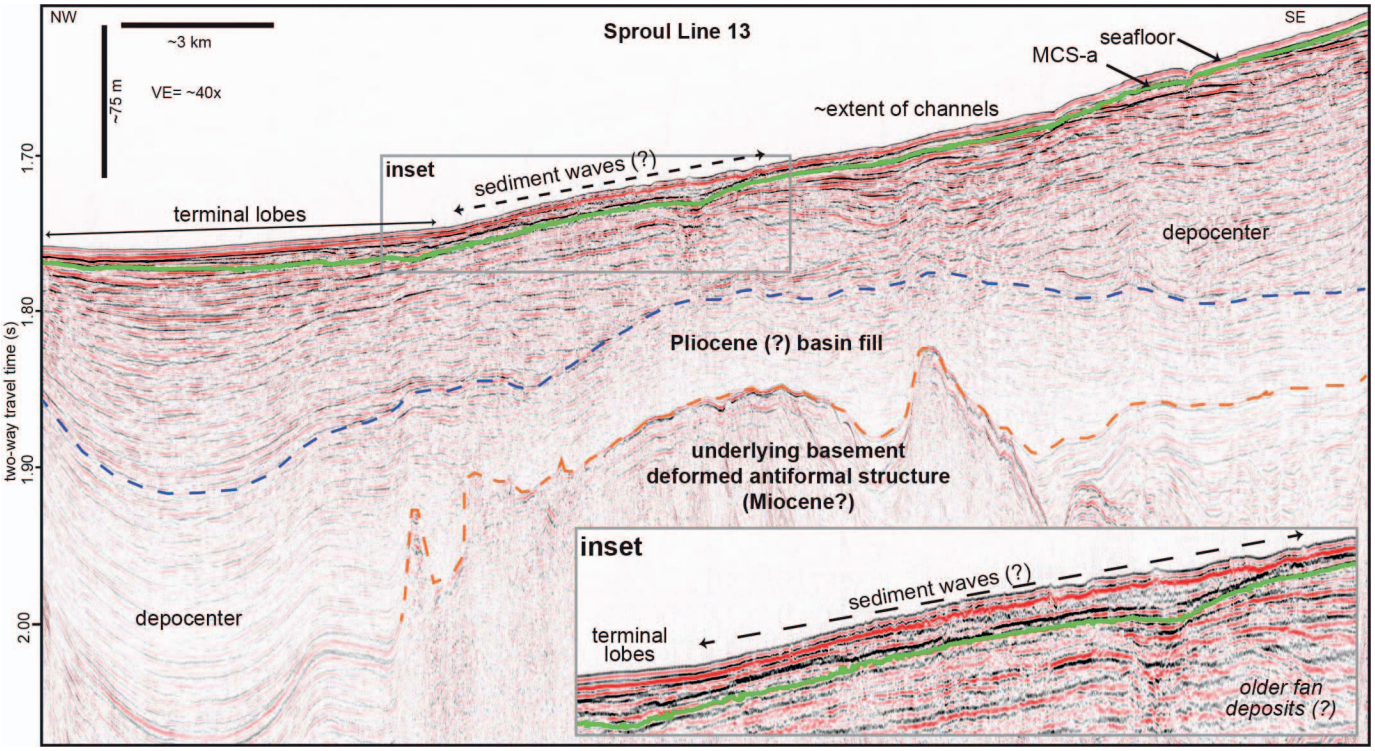

FIG. 14.—Multichannel seismic-reflection profile shows a buried basement high (deformed antiformal structure) below where a transition occurs on the seafloor from narrow, apparently disconnected channels to lobes. This underlying structure may influence seafloor gradient and the location of persistent depocenters in basin fill. See Figure 1A for profile location.

incised channels through up-dip propagation of knickpoints (e.g., Graham and Bachman 1983; Heiniö and Davies 2007). Similar disconnected (i.e., headless) channels occur on Monterey Fan and Navy Fan, where flows reincised between seamounts and shape of the fan was influenced by the underlying morphology (Normark 1985; Normark et al. 1983; Fildani and Normark 2004; Klaucke et al. 2004).

Likewise, the transition from narrow channels with knickpoints to possible small-scale sediment waves occurs at the apex of a buried and deformed antiformal structure that plunges to the north across the mid-basin and corresponds with variations in seafloor gradient (Fig. 14). Sediment-wave height is limited by flow depth and scales to sediment wavelength (e.g., Normark et al. 1980; Wynn et al. 2000a), so flows that significantly thinned as they spread across the basin would not be capable of producing sediment waves with wave heights on the order of hundreds of meters or wavelengths of kilometers. Alternatively, Symons et al. (2016) associated small-scale sediment waves (20–200 m wavelength) with coarse-grained, confined settings. The small-scale sediment waves in Catalina Basin (Fig. 10) and the Navy Fan (Carvajal et al. 2017) may be linked to confinement provided by the basin margins, faults, and other Borderland structures, representing a different type of confined depositional environment for small-scale sediment waves.

Lobes also occur down-dip from the buried antiformal structure, where a slight break in seafloor gradient occurs (from $\sim$ 0.2–0.3° to $<$ 0.1°; Fig. 3), and appear to be the latest deposition in a long-lived depocenter (e.g., Fig. 14). Interpreted lobe deposits are vertically stacked in thick successions in the depocenter (Figs. 4, 12, 14), in contrast to lateral compensation that characterizes non-tectonically controlled CLTZs and deep-sea fans (e.g., Prélat et al. 2009, 2010; Picot et al. 2016). This style of stacked depocenters and channels adjacent to structural highs may be characteristic of CLTZs in complex and confined tectonic settings (Fig. 15) (e.g., Normark 1985; Graham and Bachman 1983; Remacha et al. 2005; Liu et al. 2018).

Quaternary-active faults also may have influenced the CLTZ. Although age control is needed to analyze the relative timing of deposition and fault motion, movement along the San Clemente Fault and Catalina Fault (e.g., Legg et al. 2004a) could have altered channel thalweg gradients at the basin margins and triggered up-dip propagation of knickpoints to form apparently disconnected channels. The San Gabriel Channel enters the Catalina Basin across the dextral strike-slip San Diego Trough Fault Zone (SDTFZ), and motion along this fault ($\sim$ 1.2–1.8 mm/yr in the late Pleistocene and Holocene; Ryan et al. 2012) may have created knickpoints (Fig. 3B) and opened the basin to terrestrially derived sediment from the San Gabriel Channel. Back-slipping along the SDTFZ using the late Pleistocene slip-rate estimate suggests that the Catalina Basin may have been blocked by basement highs before $\sim$ 3 Ma. Such a hypothesized change in sediment supply, driven by fault motion and (or) extension of the San Gabriel Channel to the Catalina Basin, may be linked to the unconformity and differential seismic facies between interpreted Pliocene and Pleistocene basin fill (Fig. 14) (P1 and P2 of Teng and Gorsline 1989), but sampling and absolute dating are needed to investigate further.

Offset of deep-marine sediments across strike-slip faults has long been used to reconstruct fault motion over geologic time with considerable debate on cross-fault correlations (i.e., piercing points) (e.g., Howell et al. 1974, 1975; Cole et al. 1975; Graham et al. 1989; Sharman et al. 2013). Using deep-marine deposits as piercing points over geologic time is complex if deposition was post- and (or) syn-tectonic because sediment density flows interact with structurally controlled seafloor gradients and may not deposit fans with uniform provenance across a fault or basin (e.g., Normark 1985; Hodgson and Haughton 2004). The locus of fan deposition from the San Gabriel Channel is largely fault-parallel and ponded along the basin-bounding faults such that potential cross-fault provenance variations

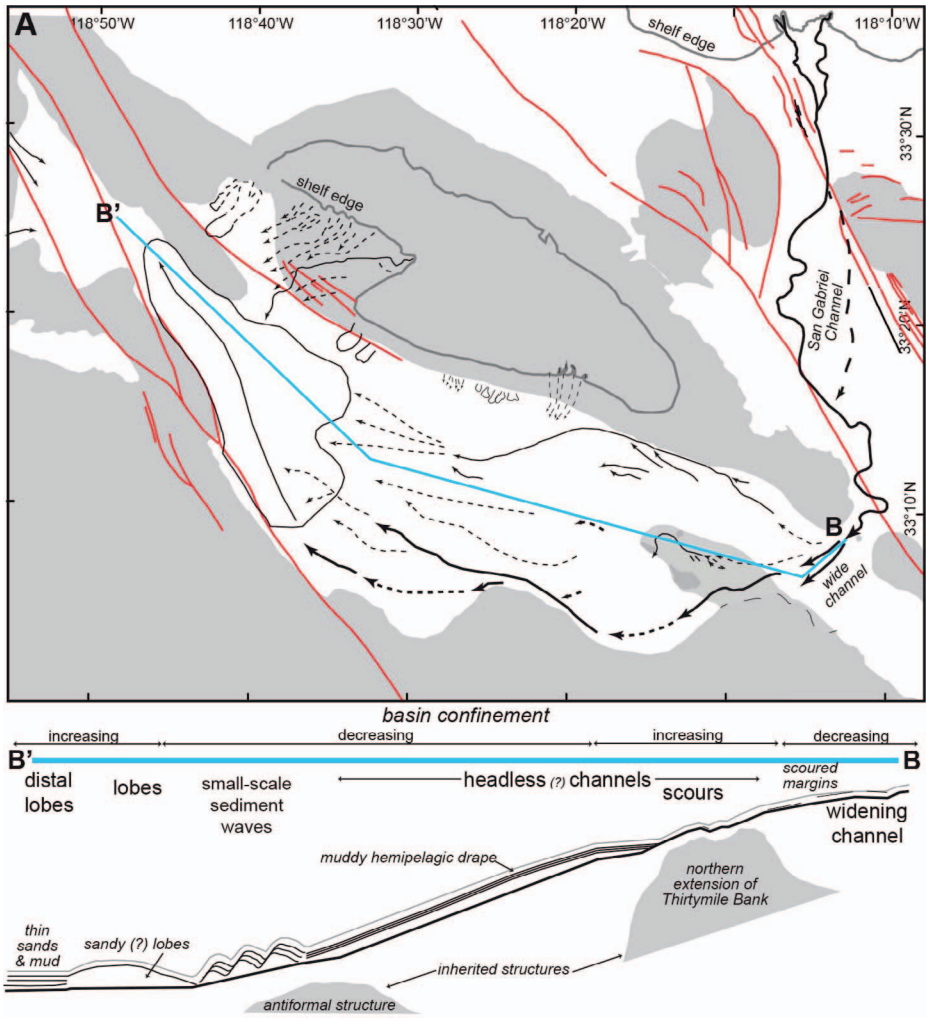

FIG. 15.—Schematic representation of channel to lobe zonation in the Catalina Basin. **A)** Map-view representation of interpreted paleoflow paths in the late Pleistocene fan package above the MCS-a horizon, with sediment from the San Gabriel Canyon–Channel and local sources (solid and bold arrows, primary pathways; dashed arrows, secondary). Shaded gray, inherited basement structures. Red lines, Quaternary-active faults, as in Figure 1. **B)** Schematic cross-sectional interpretation of the San Gabriel channel–lobe transition zone in the Catalina Basin. Approximate regions of decreasing and increasing confinement from basin geometry and underlying structure are shown above. Scale not implied.

are not related to lateral fault offset over time. Although we can map this clearly on the modern seafloor, such complex geometries would be difficult to distinguish in outcrops, even if scales of depositional features are similar (e.g., Normark 1985; Mutti and Normark 1987). Thus, this study illustrates the complex interaction and juxtaposition of active faulting, inherited structures, and deep-marine sedimentation from local and distant sources, and it could provide a modern analog or cautionary example for reconstructions over geologic time.

Comparison with Other Channel–Lobe Transition Zones

Morphologic similarities between CLTZ examples and conceptual models support common controls and inherent features of CLTZs (e.g., Wynn et al. 2002; Prélat et al. 2009, 2010; Macdonald et al. 2011; Dorrell et al. 2016; Postma et al. 2016; Brooks et al. 2018). However, CLTZs are largely identified from their location within a single depositional system; specifically, CLTZs are regions separating "well-defined channels or channel fill deposits from well-defined lobes or lobe facies" (Mutti and Normark 1987; p. 22). This definition poses continuing challenges (1) to generate data covering entire CLTZs with resolution sufficient to define small-scale channels, lobes, and intermediate morphologies in seafloor settings, and (2) to determine along-system context in outcrop studies. In particular, CLTZs have been distinguished from other weakly confined settings where deep-marine channels decrease in confinement and contain similar scours, sediment waves, and widening channels, but do not result in terminal lobes (e.g., Maier et al. 2011, 2012, 2013). Notably, sediment waves and scours are prevalent elements across deep-sea depositional systems (e.g., Symons et al. 2016; Covault et al. 2017; Hofstra et al. 2018).

Dorrell et al. (2016) note that modern seafloor CLTZ examples typically include features at different scales, and from less tectonically active settings, than outcrop CLTZ examples. The San Gabriel depositional system in the Catalina Basin provides a CLTZ example from a seafloor dataset in a relatively confined setting along a tectonically active margin with both inherited structures and active faults. The San Gabriel Channel crossing the San Diego Trough Fault into the Catalina Basin displays widening and decreasing relief with striking similarity to the Navy Fan CLTZ, where it crosses the San Clemente Fault (Carvajal et al. 2017). Channels that widen as they decrease in relief, increase in aspect ratio, and develop scoured margins may be a common feature of proximal CLTZs that cross an active fault and tectonic confinement (e.g., Fig. 7); alternatively, these features may be a broader characteristic where channel confinement decreases. Outcrop CLTZ studies (e.g., Hodgson and Haughton 2004; Remacha et al. 2005; Bernhardt et al. 2011) document flow diversion, ponding of sheet-like lobes, and tectonically controlled depositional fairways that are similar to those interpreted in Catalina Basin.

Comparison of this seafloor CLTZ with studies of outcrop CLTZs is complicated by different scales and focuses of the datasets (e.g., Mutti and Normark 1987; Normark et al. 1993). Where outcrop studies have documented channels and scours of scale similar to those in the Catalina Basin, outcrop studies may provide insights into paleoflow processes where

seafloor datasets lack samples. In particular, studies of outcrop CLTZs highlight the importance of multiple flows and headward erosion in forming and filling scours (Hofstra et al. 2015; Pemberton et al. 2016), as interpreted in the Catalina Basin scour field (e.g., Fig. 9). Pemberton et al. (2016) interpret channels developing from discontinuous scours, as may have occurred in the Catalina Basin. However, they note wide, high-aspect-ratio channels that are significantly narrower than the wide channel in the Catalina Basin. Conversely, imaging of the complete CLTZ in the Catalina Basin may serve as a seafloor analog for outcrop CLTZ interpretations that lack plan-view context.

Other seafloor examples used by Wynn et al. (2002) link CLTZ formation and regions of scours and sediment waves to breaks in slope angle. These scours and sediment waves may be cyclic steps, recently summarized by Covault et al. (2017) as common in regions of high gradients and slope breaks, or they may contain unresolved bed-scale sub-critical components (e.g., Hofstra et al. 2018). In the Catalina Basin, channel confinement is linked to tectonic confinement more than a base of slope gradient break, and small increases in gradient are linked to the possible development of sediment waves and lobes farther down-system. As available seafloor data resolution increases, our ability to resolve small-scale sediment waves, diverse scour morphologies, and subtle gradient breaks also improves (e.g., Macdonald et al. 2011; Maier et al. 2011; Carvajal et al. 2017). Erosional lineations imaged by Wynn et al., (2002) may be similar to the narrow, disconnected channels or scoured channels imaged in the Catalina Basin (Figs. 1, 9) and noted at a larger scale in Monterey Fan (Normark 1985; Klauke et al. 2004). More modern high-resolution CTLZ datasets are needed to further characterize depositional processes and evaluate trends.

We suggest that the San Gabriel CLTZ in the Catalina Basin may represent an end-member example of a CLTZ strongly influenced by tectonics, including antecedent basement topography and active faults (Fig. 15). The morphologies, size, and sequence of features documented in the Catalina Basin may be characteristic of tectonically controlled CLTZs (Fig. 15). The most important aspect of the tectonic end member presented here may be tectonic restriction provided by basement highs and fault-controlled basin margins that resulted in consistent stacking of depocenters (e.g. Fig. 14), prevented channel avulsion through the Pleistocene, determined geometry of lobes and basin fill, and may have restricted CLTZ location through time.

CONCLUSIONS

This study uses comprehensive high-resolution imaging across Catalina Basin to analyze a complete channel–lobe transition zone on the modern seafloor formed in a tectonically active, confined basin setting. Sedimentation in the Catalina Basin is dominated by the San Gabriel sediment source that appears to have shut off during post-Last Glacial Maximum sea-level rise. Late Pleistocene sediment and seafloor morphology in the Catalina Basin contain a channel–lobe transition zone, including a zone of scours, narrow and apparently disconnected channels with knickpoints, and possible unusually small-scale sediment waves between the confined San Gabriel Channel and its terminal lobes $>$ 50 km into the basin. The San Gabriel Channel initially widens and develops scoured edges as it enters the Catalina Basin. The San Gabriel channel–lobe transition zone in the Catalina Basin is considered here an end-member example of a channel–lobe transition zone because the confined channel is locked between basement highs such that channel avulsion appears to be prohibited (now and possibly through the Pleistocene). Locations of, and increased gradient related to, inherited basement structures are associated with changes in channel confinement, the scour field, narrow disconnected channels with knickpoints, and sediment waves. These basement structures have concentrated channels and stacked lobes in depocenters along areas of decreased gradient in the basin and along structurally controlled basin margins. Common features imaged in this and other channel–lobe transition zones suggest some common processes across channel–lobe transition zones. However, in this tectonically complex setting, the locations of CLTZ components are linked to underlying basement structure, faults, and basin margins. Comprehensive characterization of this channel–lobe transition zone may provide an analog for larger seafloor examples with incomplete imaging across tectonically active margins, and for outcrop studies lacking plan-view morphology.

ACKNOWLEDGEMENTS

Research cruise 2014-645-FA aboard the R/V *Sproul* was funded by the US Geological Survey Coastal and Marine Program (CMG) and received additional support from the University of California Ship Funds Program. Research cruise 2016-616-FA aboard the R/V *Thompson* was funded by the University of Washington with additional support from USGS CMG. We thank Jackson Currie, Rob Wyland, Chuck Worley, Tommy O'Brien, Emily Wei, Lana Graves, and the research-vessel crews for their assistance in data acquisition; Pat Hart, Alicia Balster-Gee, and Dan Ebuna for geophysical data acquisition and processing; and Matthew Malkowski for helpful discussions. We thank Cristian Carvajal, Kirt Campion, Tim McHargue, and Associate Editor Morgan Sullivan for helpful reviews of this manuscript. We are grateful to John Southard for copy editing. Any use of trade, product, or firm names is for descriptive purposes only and does not imply endorsement by the U.S. Government.

REFERENCES

Alexander, C.R., and Lee, H.J., 2009, Sediment accumulation on the Southern California Bight continental margin during the twentieth century, *in* Lee, H.J., and Normark, W.R., eds., Earth Science in the Urban Ocean: The Southern California Continental Borderland: Geological Society of America, Special Paper 454, p. 69–87.

Babonneau, N., Savoye, B., Cremer, M., and Klein, B., 2002, Morphology and architecture of the present canyon and channel system of the Zaire deep-sea fan: Marine and Petroleum Geology, v. 19, p. 445–467.

Bennett, R.A., Rodi, W., and Reilinger, R.E., 1996, Global Positioning System constraints on fault slip rates in southern California and northern Baja, Mexico: Journal of Geophysical Research, Solid Earth, v. 101, p. 21,943–21,960.

Bernhardt, A., Jobe, Z.R., and Lowe, D.R., 2011, Stratigraphic evolution of a submarine channel–lobe complex system in a narrow fairway within the Magallanes foreland basin, Cerro Toro Formation, southern Chile: Marine and Petroleum Geology, v. 28, p. 785–806, doi: 10.1016/j.marpetgeo.2010.05.013.

Bohannon, R.G., and Geist, E., 1998, Upper crustal structure and Neogene tectonic development of the California continental borderland: Geological Society of America, Bulletin, v. 110, p. 779–800.

Bonnel, C., Dennielou, B., Droz, L., Mulder, T., and Berné, S., 2005, Architecture and depositional pattern of the Rhône Neofan and recent gravity activity in the Gulf of Lions (western Mediterranean): Marine and Petroleum Geology, v. 22, p. 827–843.

Brandsma, D., Lund, S.P., and Henyey, T.L., 1989, Paleomagnetism of late Quaternary marine sediments from Santa Catalina Basin, California Continental Borderland: Journal of Geophysical Research, v. 94, p. 547–564.

Brooks, H.L., Hodgson, D.M., Brunt, R.L., Peakall, J., Hofstra, M., and Flint, S.S., 2018, Deep-water channel–lobe transition zone dynamics: processes and depositional architecture, an example from the Karoo Basin, South Africa: Geological Society of America, Bulletin, doi:10.1130/B31714.1.

Buffington, E.C., 1964, Structural control and precision bathymetry of La Jolla submarine canyon, California: Marine Geology, v. 1, p. 44–58.

Carvajal, C., Paull, C.K., Caress, D.W., Fildani, A., Lundsten, E., Anderson, K., Maier, K.L., McGann, M., Gwiazda, R., and Herguera, J.C., 2017, Unraveling the channel–lobe transition zone with high-resolution AUV bathymetry: Navy Fan, offshore Baja California, Mexico: Journal of Sedimentary Research, v. 87, p. 1049–1059, doi:10.2110/jsr.2017.58.

Chang, S.-K., and Douglas, R.G., 1987, Holocene turbidites of Santa Catalina Basin, California continental borderland: Geological Society of Korea, Journal, v. 23, p. 16–31 (abstract in English).

Cole, M.R., Merschat, W.R., and Parsley, R.M., 1975, Possible strike-slip faulting in the Southern California Borderland: Comment: Geology, v. 3, p. 2–3.

Covault, J.A., and Romans, B.W., 2009, Growth patterns of deep-sea fans revisited: turbidite-system morphology in confined basins, examples from the California Borderland: Marine Geology, v. 265, p. 51–66.

Covault, J.A., Kostic, S., Paull, C.K., Ryan, H.F., and Fildani, A., 2014, Submarine channel initiation, filling and maintenance from sea-floor geomorphology and morphodynamic modelling of cyclic steps: Sedimentology, v. 61, p. 1031–1054, doi:10.1111/sed.12084.

Covault, J.A., Kostic, S., Paull, C.K., Sylvester, Z., and Fildani, A., 2017, Cyclic steps and related supercritical bedforms: building blocks of deep-water depositional systems,

western North America: Marine Geology, v. 393, p. 4–20, doi:10.1016/j.margeo.2016.12.009.

Crouch, J.K., 1981, Northwest margin of California Continental Borderland: marine geology and tectonic evolution: American Association of Petroleum Geologists, Bulletin, v. 65, p. 191–218.

Crouch, J.K., and Suppe, J., 1993, Late Cenozoic tectonic evolution of the Los Angeles basin and inner California borderland: a model for core complex-like crustal extension: Geological Society of America, Bulletin, v. 105, p. 1415–1434.

Dartnell, P., Driscoll, N.W., Brothers, D., Conrad, J.E., Kluesner, J., Kent, G., and Andrews, B., 2015, Color shaded-relief bathymetry, acoustic backscatter, and selected perspective views of the inner continental borderland, Southern California, U.S. Geological Survey Scientific Investigations Map 3324, 2 sheets, http://dx.doi.org/10.3133/sim3324.

Dartnell, P., Roland, E.C., Raineault, N.A., Castillo, C.M., Conrad, J.E., Kane, R.R., Brothers, D.S., Kluesner, J.W., and Walton, M.A.L., 2017, Multibeam bathymetry and acoustic-backscatter data collected in 2016 in Catalina Basin, southern California and merged multibeam bathymetry datasets of the northern portion of the Southern California Continental Borderland: U.S. Geological Survey, Data Release, https://doi.org/10.5066/F7DV1H3W.

DeMets, C., Gordon, R.G., and Argus, D.F., 2010, Geological current plate motions: Geophysical Journal International, v. 181, p. 1–80.

Dorrell, R.M., Peakall, J., Sumner, E.J., Parsons, D.R., Darby, S.E., Wynn, R.B., Özsoy, E., and Tezcan, D., 2016, Flow dynamics and mixing processes in hydraulic jump arrays: implications for channel–lobe transition zones: Marine Geology, v. 381, p. 181–193, doi:10.1016/j.marpetgeo.2016.09.009.

Emery, K.L., 1960, The Sea off Southern California: A Modern Habitat of Petroleum: New York, John Wiley & Sons, 366 p.

Emery, K.O., and Bray, E.E., 1962, Radiocarbon dating of California Basin Sediments: American Association of Petroleum Geologists, Bulletin, v. 46, p. 1839–1856.

Ercilla, G., Casas, D., Estrada, F., Váquez, J.T., Iglesias, J., García, M., Gómez, M., Acosta, J., Gallart, J., Maestro-González, A., and Marconi Team, 2008a, Morphosedimentary features and recent depositional architectural model of the Cantabrian continental margin: Marine Geology, v. 247, p. 61–83, doi:10.1016/j.margeo.2007.08.007.

Ercilla, G., Iglesias, J., Casas, D., Estrada, F., Váquez, J.T., García, M., Gómez, M., and MARCONI Team, 2008b, Recent sedimentary processes on the Cantabrian continental margin, eastern Bay of Biscay: Geo-Temas, v. 10, p. 515–518.

Fisher, M.A., Langenheim, V.E., Nicholson, C., Ryan, H.F., and Sliter, R.W., 2009, Recent developments in understanding the tectonic evolution of the Southern California offshore area, *in* Lee, H.J., and Normark, W.R., eds., Implications for Earthquake-Hazard Analysis: Geological Society of America, Special Paper 454, p. 229–250.

Fildani, A., and Normark, W.R., 2004, Late Quaternary evolution of channel and lobe complexes of Monterey Fan: Marine Geology, v. 206, p. 199–223.

Fildani, A., Normark, W.R., Kostic, S., and Parker, G., 2006, Channel formation by flow stripping: large-scale scour features along the Monterey East Channel and their relation to sediment waves: Sedimentology, v. 53, p. 1265–1287.

Fildani, A., Hubbard, S.M., Covault, J.A., Maier, K.L., Romans, B.W., Traer, M., and Rowland, J.C., 2013, Erosion at inception of deep-sea channels: Marine and Petroleum Geology, v. 41, p. 48–61.

Gaal, R.A.P., 1966, Marine Geology of the Santa Catalina Basin Area, California [Ph.D. Dissertation]: University of Southern California, 268 p.

Gardner, J.V., Dartnell, P., Mayer, L.A., and Hughes Clarke, J.E., 2003, Geomorphology, acoustic backscatter, and processes in Santa Monica Bay from multibeam mapping: Marine Environmental Research, v. 56, p. 15–46, doi:10.1016/S0141-1136(02)00323-9.

Graham, S.A., and Bachman, S.B., 1983, Structural controls on submarine-fan geometry and internal architecture: Upper La Jolla Fan System, offshore Southern California: American Association of Petroleum Geologists, Bulletin, v. 67, p. 83–96.

Graham, S.A., Stanley, R.G., Bent, J.V., and Carter, J.B., 1989, Oligocene and Miocene paleogeography of central California and displacement along the San Andreas fault: Geological Society of America, Bulletin, v. 101, p. 711–730.

Gervais, A., Savoye, B., Mulder, T., and Gonthier, E., 2006, Sandy modern turbidite lobes: a new insight from high resolution seismic data: Marine and Petroleum Geology, v. 23, p. 485–502.

Grecula, M., Flint, S., Potts, G., Wickens, D., and Johnson, S., 2003, Partial ponding of turbidite systems in a basin with subtle growth-fold topography: Laingsburg–Karoo, South Africa: Journal of Sedimentary Research, v. 73, p. 603–620.

Heiniö, P., and Davies, R.J., 2007, Knickpoint migration in submarine channels in response to fold growth, western Niger Delta: Marine and Petroleum Geology, v. 24, p. 434–449, doi:10.1016/j.marpetgeo.2006.09.002.

Hodgson, D.M., and Haughton, P.D.W., 2004, Impact of syndepositional faulting on gravity current behaviour and deep-water stratigraphy: Tabernas–Sorbas Basin, SE Spain, *in* Lomas, S.A., and Joseph, P., eds., Confined Turbidite Systems: Geological Society of London, Special Publication 222, p. 135–158, doi:10.1144/GSL.SP.2004.01.08.

Hofstra, M., Hodgson, D.M., Peakall, J., and Flint, S.S., 2015, Giant scour-fills in ancient channel–lobe transition zones: formative processes and depositional architecture: Sedimentary Geology, v. 329, p. 98–114, doi: 10.1016.j.sedgeo.2015.09.004.

Hofstra, M., Peakall, J., Hodgson, D.M., and Stevenson, C.J., 2018, Architecture and morphodynamics of subcritical sediment waves in an ancient channel–lobe transition zone: Sedimentology, doi:10.1111/sed.12468.

Howell, D.G., Stuart, C.J., Platt, J.P., and Hill, D.J., 1974, Possible strike-slip faulting in the Southern California Borderland: Geology, v. 2, p. 93–98.

Howell, D.G., Stuart, C.J., Platt, J.P., and Hill, D.J., 1975, Possible strike-slip faulting in the Southern California Borderland: Reply: Geology, v. 3, p. 3–4.

Jegou, I., Savoye, B., Pirmez, C., and Droz, L., 2008, Channel-mouth lobe complex of the recent Amazon Fan: the missing piece: Marine Geology, v. 252, p. 62–77.

Klaucke, I., Masson, D.G., Kenyon, N.H., and Gardner, J.V., 2004, Sedimentary processes of the lower Monterey Fan channel and channel-mouth lobe: Marine Geology, v. 206, p. 181–198.

Kuang, Z., Zhong, G., Wang, L., and Guo, Y., 2014, Channel-related sediment waves on the eastern slope offshore Dongsha Islands, northern South China Sea: Journal of Asian Earth Sciences, v. 79, p. 540–551, doi:10.1016/j.jseaes.2012.09.025.

Lambeck, K., and Chappell, J., 2001, Sea level change through the Last Glacial Cycle: Science, v. 292, p. 679–686, doi:10.1126/science.1059549.

Legg, M.R., 1991, Development in understanding the tectonic evolution of the California Continental Borderland, *in* Normark, W.R., and Piper, D.J.W., eds., Shoreline to Abyss: Contributions in Marine Geology in Honor of Francis P. Shepard: SEPM, Special Publication 46, p. 291–312.

Legg, M.R., Borrero, J.C., and Synolakis, C.E., 2004a, Tsunami Hazards Associated with the Catalina Fault in Southern California: Earthquake Spectra, v. 20, p. 917–950.

Legg, M.R., Nicholson, C., Goldfinger, C., Milstein, R., and Kamerling, M.J., 2004b, Large enigmatic crater structures offshore southern California: Geophysical Journal International, v. 159, p. 803–815.

Legg, M.R., Goldfinger, C., Kamerling, M.J., Chaytor, J.D., and Einstein, D.E., 2007, Morphology, structure and evolution of California Continental Borderland restraining bends, *in* Cunningham, W.D., and Mann, P., eds., Tectonics of Strike-Slip Restraining and Releasing Bends: Geological Society of London, Special Publication 290, p. 143–168.

Legg, M.R., Kohler, M.D., Shintaku, N., and Weeraratne, D.S., 2015, High-resolution mapping of two large-scale transpressional fault zone in the California Continental Borderland: Santa Cruz–Catalina Ridge and Ferrelo faults: Journal of Geophysical Research, Earth Surface, v. 120, p. 915–942, doi:10.1002/2014JF003322.

Liu, Q., Kneller, B., Fallgatter, C., Valdez Buso, V., and Milana, J.P., 2018. Tabularity of individual turbidite beds controlled by flow efficiency and degree of confinement: Sedimentology, doi:10.1111/sed.12470.

Lomas, S.A., and Joseph, P., 2004, Confined Turbidite Systems, *in* Lomas, S.A., and Joseph, P., eds., Confined Turbidite Systems: Geological Society of London, Special Publication 222, p. 1–7.

Macdonald, H.A., Wynn, R.B., Huvenne, V.A.I., Peakall, J., Masson, D.G., Weaver, P.P.E., and McPhail, S.D., 2011, New insights into the morphology, fill, and remarkable longevity (>0.2 m.y.) of modern deep-water erosional scours along the northeast Atlantic margin: Geosphere, v. 7, p. 845–867.

Maier, K.L., Fildani, A., Paull, C.K., Graham, S.A., McHargue, T.R., Caress, D.W., and McGann, M., 2011, The elusive character of discontinuous deep-water channels: new insights from Lucia Chica channel system, offshore California: Geology, v. 39, p. 327–330.

Maier, K.L., Fildani, A., McHargue, T., Paull, C.K., Graham, S.A., and Caress, D.W., 2012, Punctuated deep-water channel migration: high-resolution subsurface data from the Lucia Chica channel system, offshore California, U.S.A.: Journal of Sedimentary Research, v. 82, p. 1–8.

Maier, K.L., Fildani, A., Paull, C.K., McHargue, T.R., Graham, S.A., and Caress, D.W., 2013, Deep-sea channel evolution and stratigraphic architecture from inception to abandonment from high-resolution Autonomous Underwater Vehicle surveys offshore central California: Sedimentology, v. 60, p. 935–960.

Maier, K.L., Brothers, D.S., Paull, C.K., McGann, M., Caress, D.W., and Conrad, J.E., 2017, Records of continental slope sediment flow morphodynamic responses to gradient and active faulting from integrated AUV and ROV data, offshore Palos Verdes, southern California Borderland: Marine Geology, v. 393, p. 47–66, doi:10.1016/j.margeo.2016.10.001.

Marini, M., Patacci, M., Felletti, F., and McCaffrey, W.D., 2016, Fill to spill stratigraphic evolution of a confined turbidite mini-basin succession, and its likely well bore expression: the Castagnola Fm, NW Italy: Marine and Petroleum Geology, v. 69, p. 94–111, doi:10.1016/j.marpetgeo.2015.10.014.

Maslin, M., Knutz, P.C., and Ramsay, T., 2006, Millennial-scale sea-level control on avulsion events on the Amazon Fan: Quaternary Science Reviews, v. 25, p. 3338–3345.

McHargue, T., Pyrcz, M.J., Sullivan, M.D., Clark, J.D., Fildani, A., Romans, B.W., Covault, J.A., Levy, M., Posamentier, H.W., and Drinkwater, N.J., 2011, Architecture of turbidite channel systems on the continental slope: patterns and predictions: Marine and Petroleum Geology, v. 28, p. 728–743.

Moore, D.G., 1969, Reflection profiling studies of the California Continental Borderland: Structure and Quaternary turbidite basins: Geological Society of America, Special Paper 107, 142 p.

Mutti, E., and Normark, W.R., 1987, Comparing examples of modern and ancient turbidite systems: problems and concepts, *in* Leggett, J.K., and Zuffa, G.G., eds., Marine Clastic Sedimentology: Concepts and Case Studies: London, Graham and Trotman, p. 1–38.

Nicholson, C., Sorlien, C.C., Atwater, T., Crowell, J.C., and Luyendyk, B.P., 1994, Microplate capture, rotation of the western Transverse Ranges, and initiation of the San Andreas transform as a low-angle fault system: Geology, v. 22, p. 491–495.

Normark, W.R., 1970, Growth patterns of deep-sea fans: American Association of Petroleum Geologists, Bulletin, v. 54, p. 2170–2195.

Normark, W.R., 1985, Local morphologic controls and effects of basin geometry on flow processes in deep marine basins, *in* Zuffa, G.G., ed., Provenance of Arenites: Springer, Dordrecht, p. 47–63.

Normark, W.R., Piper, D.J.W., and Hess, G.R., 1979, Distributary channels, sand lobes, and mesotopography of Navy Submarine Fan, California Borderland, with applications to ancient fan sediments: Sedimentology, v. 26, p. 749–774.

Normark, W.R., Hess, G.R., Stow, D.A.V., and Bowen, A.J., 1980, Sediment waves on the Monterey fan levee: a preliminary physical interpretation: Marine Geology, v. 37, p. 1–18.

Normark, W.R., Gutmacher, C.E., Chase, T.E., and Wilde, P., 1983, Monterey Fan: growth pattern control by basin morphology and changing sea levels: Geo-Marine Letters, v. 3, p. 93–99.

Normark, W.R., Posamentier, H., and Mutti, E., 1993, Turbidite systems: state of the art and future directions: Reviews of Geophysics, v. 31, p. 91–116.

Normark, W.R., Piper, D.J.W., and Hiscott, R.M., 1998, Sea level controls on the textural characteristics and depositional architecture of the Hueneme and associated submarine fan systems, Santa Monica Basin, California: Sedimentology, v. 45, p. 53–70.

Normark, W.R., Baher, S., and Sliter, R., 2004, Late Quaternary sedimentation and deformation in Santa Monica and Catalina Basins, offshore southern California, *in* Legg, M.R., Davis, P., and Gath, E., eds., Geology and Tectonics of Santa Catalina Island and the California Continental Borderland: South Coast Geological Society, Santa Ana, California, Field Trip Guidebook 32, p. 291–317.

Normark, W.R., McGann, M., and Sliter, R., 2009a, Late Quaternary sediment-accumulation rates within the inner basins of the California Continental Borderland in support of geologic hazard evaluation, *in* Lee, H.J., and Normark, W.R., eds., Earth Science in the Urban Ocean: The Southern California Continental Borderland: Geological Society of America, Special Paper 454, p. 117–139.

Normark, W.R., Piper, D.J.W., Romans, B.W., Covault, J.A., Dartnell, P., and Sliter, R.W., 2009b, Submarine canyon and fan systems of the California Continental Borderland, *in* Lee, H.J., and Normark, W.R., eds., Earth Science in the Urban Ocean: The Southern California Continental Borderland: Geological Society of America, Special Paper 454, p. 141–168.

O'Connell, S., and Normark, W.R., 1986, 20. Acoustic facies and sediment composition of the Mississippi Fan drill sites, Deep Sea Drilling Project Leg 96, *in* Bouma, A.H., Coleman, J.M., and Meyer, A.W., eds., Initial Reports of the Deep Sea Drilling Project Volume XCVI: Washington, D.C., U.S. Government Printing Office, p. 457–473.

Ortiz-Karpf, A., Hodgson, D.M., and McCaffrey, W.D., 2015, The role of mass-transport complexes in controlling channel avulsion and the subsequent sediment dispersal patterns on an active margin: the Magdalena Fan, offshore Colombia: Marine and Petroleum Geology, v. 64, p. 58–75.

Pemberton, E.A.L., Hubbard, S.M., Fildani, A., Romans, B., and Stright, L., 2016, The stratigraphic expression of decreasing confinement along a deep-water sediment routing system: outcrop example from southern Chile: Geosphere, v. 12, p. 114–134, doi:10.1130/GES01233.1.

Picot, M., Droz, L., Marsset, T., Dennielou, B., and Bez, M., 2016, Controls on turbidite sedimentation: insights from a quantitative approach of submarine channel and lobe architecture (late Quaternary Congo Fan): Marine and Petroleum Geology, v. 72, p. 423–446, doi:10.1016/j.marpetgeo.2016.02.004.

Piper, D.J.W., and Normark, W.R., 2001, Sandy fans: from Amazon to Hueneme and beyond: American Association of Petroleum Geologists, Bulletin, v. 85, p. 1407–1438.

Platt, J.P., and Becker, T.W., 2010, Where is the real transform boundary in California?: Geochemistry, Geophysics, Geosystems, v. 11, no. Q06012.

Postma, G., Hoyal, D.C., Abreu, V., Cartigny, M.J.B., Demko, T., Fedele, J.J., Kleverlaan, K., and Pederson, K.H., 2016, Morphodynamics of supercritical turbidity currents in the channel–lobe transition zone: Submarine Mass Movements and their Consequences, v. 41, p. 469–478.

Prather, B.E., Booth, J.R., Steffens, G.S., and Craig, P.A., 1998, Classification, lithologic calibration, and stratigraphic succession of seismic facies of intraslope basins, deep-water Gulf of Mexico: American Association of Petroleum Geologists, Bulletin, v. 82, p. 701–728.

Prélat, A., Hodgson, D.M., and Flint, S.S., 2009, Evolution, architecture and hierarchy of distributary deep-water deposits: a high-resolution outcrop investigation from the Permian Karoo Basin, South Africa: Sedimentology, v. 56, p. 2132–2154.

Prélat, A., Covault, J.A., Hodgson, D.M., Fildani, A., and Flint, S.S., 2010, Intrinsic controls on the range of volumes, morphologies, and dimensions of submarine lobes: Sedimentary Geology, v. 232, p. 66–76, doi:10.1016/j.sedgeo.2010.09.010.

Remacha, E., Fernández, L.P., and Maestro, E., 2005, The transition between sheet-like lobe and basin-plain turbidites in the Hecho Basin (south-central Pyrenees, Spain): Journal of Sedimentary Research, v. 75, p. 798–819, doi:10.2110/jsr.2005.064.

Richards, M., and Bowman, M., 1998, Submarine fans and related depositional systems II: variability in reservoir architecture and wireline log character: Marine and Petroleum Geology, v. 15, p. 821–839.

Romans, B.W., Normark, W.R., McGann, M.M., Covault, J.A., and Graham, S.A., 2009, Coarse-grained sediment delivery and distribution in the Holocene Santa Monica Basin, California: implications for evaluating source-to-sink flux at millennial time scales: Geological Society of America, Bulletin, v. 121, p. 1394–1408, doi:10.1130/B26393.1.

Ryan, H.F., Legg, M.R., Conrad, J.E., and Sliter, R.W., 2009, Recent faulting in the Gulf of Santa Catalina: San Diego to Dana Point, *in* Lee, H.J., and Normark, W.R., eds., Earth Science in the Urban Ocean: The Southern California Continental Borderland: Geological Society of America, Special Paper 454, p. 291–315.

Ryan, H.F., Conrad, J.E., Paull, C.K., and McGann, M., 2012, Slip rate on the San Diego Trough Fault Zone, Inner California Borderland, and the 1986 Oceanside Earthquake swarm revisited: Seismological Society of America, Bulletin, v. 102, p. 2300–2312, doi:10.1785/0120110317.

Schwalbach, J.R., and Gorsline, D.S., 1985, Holocene sediment budgets for the basins of the California Continental Borderland: Journal of Sedimentary Petrology, v. 55, p. 829–842.

Shanmugam, G., and Moiola, R.J., 1991, Types of submarine fan lobes: models and implications: American Association of Petroleum Geologists, Bulletin, v. 75, p. 156–179.

Sharman, G.R., Graham, S.A., Grove, M., and Hourigan, J.K., 2013, A reappraisal of the early slip history of the San Andreas fault, central California, USA: Geology, v. 41, p. 727–730, doi:10.1130/G34214.1.

Shaw, P.M., and Johns, R.B., 1986, The identification of organic input sources of sediments from the Santa Catalina Basin using factor analysis: Advances in Organic Geochemistry, v. 10, p. 951–958.

Shepard, F.P., Dill, R.F., and von Rad, U., 1969, Physiography and sedimentary processes of La Jolla submarine fan and fan-valley, California: American Association of Petroleum Geologists, Bulletin, v. 53, p. 390–420.

Smith, R.U., 2004, Silled sub-basins to connected tortuous corridors: sediment distribution systems on topographically complex sub-aqueous slopes, *in* Lomas, S.A., and Joseph, P., eds., Confined Turbidite Systems: Geological Society of London, Special Publication 222, p. 23–43.

Sommerfield, C.K., Lee, H.J., and Normark, W.R., 2009, Sediment accumulation on the Southern California Bight continental margin during the twentieth century, *in* Lee, H.J., and Normark, W.R., eds., Earth Science in the Urban Ocean: The Southern California Continental Borderland: Geological Society of America, Special Paper 454, p. 89–116.

Sylvester, Z., Pirmez, C., and Cantelli, A., 2011, A model of submarine channel–levee evolution based on channel trajectories: implications for stratigraphic architecture: Marine and Petroleum Geology, v. 28, p. 716–727.

Symons, W.O., Sumner, E.J., Talling, P.J., Cartigny, M.J.B., and Clare, M.A., 2016, Large-scale sediment waves and scours on the modern seafloor and their implications for the prevalence of supercritical flows: Marine Geology, v. 371, p. 130–148, doi:10.1016/j.margeo.2015.11.009.

ten Brink, U.S., Zhang, J., Brocher, T.M., Okaya, D.A., Klitgord, K.D., and Fuis, G.S., 2000, Geophysical evidence for the evolution of the California Inner Continental Borderland as a metamorphic core complex: Journal of Geophysical Research, v. 105, p. 5835–5857.

Teng, L.S., and Gorsline, D.S., 1989, Late Cenozoic sedimentation in California Continental Borderland basins as revealed by seismic facies analysis: Geological Society of America, Bulletin, v. 101, p. 27–41.

Twitchell, D.C., Schwab, W.C., Nelson, C.H., Kenyon, N.H., and Lee, H.J., 1992, Characteristics of a sandy depositional lobe on the outer Mississippi fan from SeaMARC IA sidescan sonar images: Geology, v. 20, p. 689–692.

Vedder, J.G., 1987, Regional geology and petroleum potential of the southern California Borderland, *in* Scholl, D.W., Grantz, A., and Vedder, J.G., eds., Geology and Resource-Potential of the Continental Margin of Western North America and Adjacent Ocean Basins: Beaufort Sea to Baja California: Circum-Pacific Council for Energy and Mineral Resources, v. 6, p. 403–447.

Warrick, J.A., and Farnsworth, K.L., 2009, Sources of sediment to the coastal waters of the Southern California Bight, *in* Lee, H.J., and Normark, W.R., eds., Earth Science in the Urban Ocean: The Southern California Continental Borderland: Geological Society of America, Special Paper 454, p. 39–52.

Wynn, R.B., and Stow, D.A.V., 2002, Classification and characterization of deep-water sediment waves: Marine Geology, v. 192, p. 7–22.

Wynn, R.B., Weaver, P.P.E., Ercilla, G., Stow, D.A.V., and Masson, D.G., 2000a, Sedimentary processes in the Selvage sediment-wave field, NE Atlantic: new insights into the formation of sediment waves by turbidity currents: Sedimentology, v. 47, p. 1181–1197.

Wynn, R.B., Masson, D.G., Stow, D.A.V., and Weaver, P.P.E., 2000b, Turbidity current sediment waves on the submarine slopes of the western Canary Islands: Marine Geology, v. 163, p. 185–198.

Wynn, R.B., Kenyon, N.H., Masson, D.G., Stow, D.A.V., and Weaver, P.P.E., 2002, Characterization and recognition of deep-water channel–lobe transition zones: American Association of Petroleum Geologists, Bulletin, v. 86, p. 1441–1462.

Wynn, R.B., Cronin, B.T., and Peakall, J., 2007, Sinuous deep-water channels: genesis, geometry and architecture: Marine and Petroleum Geology, v. 24, p. 341–387.

Received 18 August 2017; accepted 12 June 2018.